KITP LSMatter August 11, 2015

Topological properties and correlation effects in oxide heterostructures

Satoshi Okamoto

Materials Science and Technology Division, Oak Ridge National Laboratory

Support: the U.S. Department of Energy, Office of Science, Basic Energy Sciences, Materials Sciences and Engineering Division

OAK RIDGE National Laboratory

U.S. DEPARTMENT OF ENERGY

Outline

- **Oxide heterostructures**
- **Motivation**
- **Designing novel quantum states**
  - **Quantum spin Hall effects (DFT)**
  - **Correlation-induced Mott transition (DMFT)**
  - **Approach from Mott insulators (slave boson)**

Early work on “complex” oxide heterostructures

(Strain) control of bulk properties

Thin films of high-T_c cuprates

- I. Bozovic, *et al*. Atomic-layer engineering of cuprate superconductors, J. Supercond. **7**, 187 (1994).
- H. Sato and M. Naito, Increase in the superconducting transition temperature by anisotropic strain effect in (001) $La_{1.85}Sr_{0.15}CuO_4$ thin films on $LaSrAlO_4$ substrates, Physica C **274**, 221 (1997).

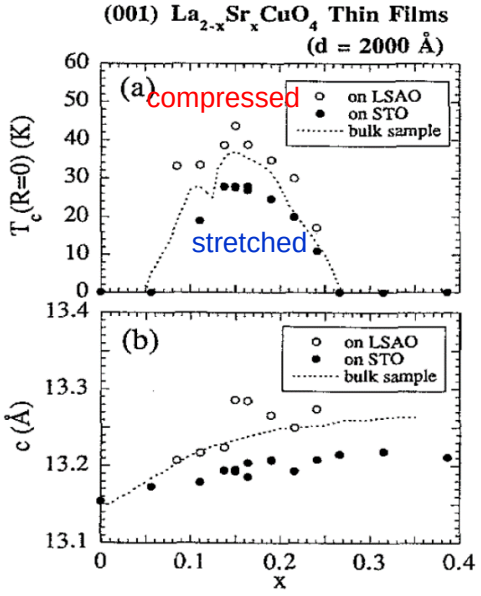

Sato & Naito

Thin films of CMR manganites

- M. Izumi, *et al*. Atomically defined epitaxy and physical properties of strained $La_{0.6}Sr_{0.4}MnO_3$ films, Appl. Phys. Lett. **73**, 2497 (1998).
- Y. Konishi, *et al*. Orbital-State-Mediated Phase-Control of Manganites, J. Phys. Soc. Jpn. **68**, 3790 (1999).

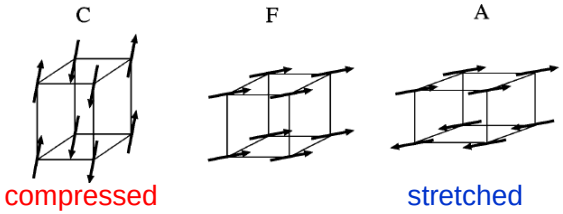

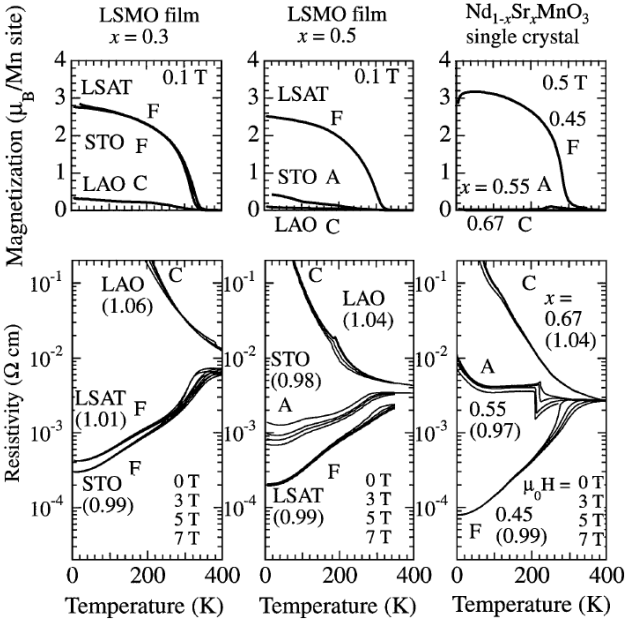

Konishi *et al*.

Work on oxide heterostructures

Exploring new electronic states: 21st century alchemy

Mott insulator ($LaTiO_3$)-band insulator ($SrTiO_3$) heterostructures

- A. Ohtomo, *et al*. Artificial charge-modulationin atomic-scale perovskite titanate superlattices, Nature **419**, 378 (2002).

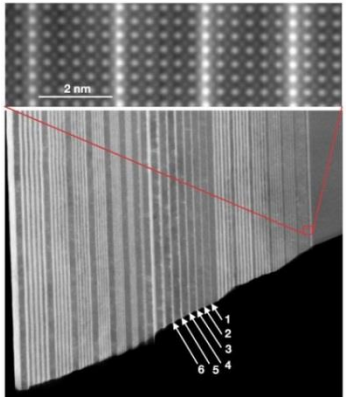

Ohtomo 2002

Band insulator² ($LaAlO_3$ and $SrTiO_3$) heterostructures

- A. Ohtomo and H. Y. Hwang, A high-mobility electron gas at the $LaAlO_3/SrTiO_3$ heterointerface, Nature **427**, 423 (2004).
- N. Nakagawa, *et al*. Why some interfaces cannot be sharp, Nature Materials **5**, 204 (2006).
- Metallic interfaces can become superconducting and magnetic (~400 papers by Web of Science from "LaAlO3/SrTiO3" and "2004-2014').

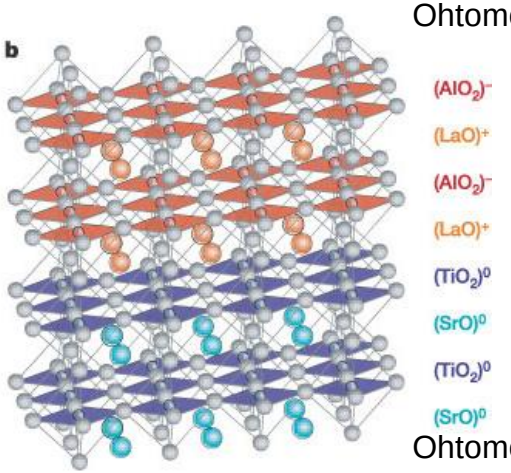

Ohtomo 2004

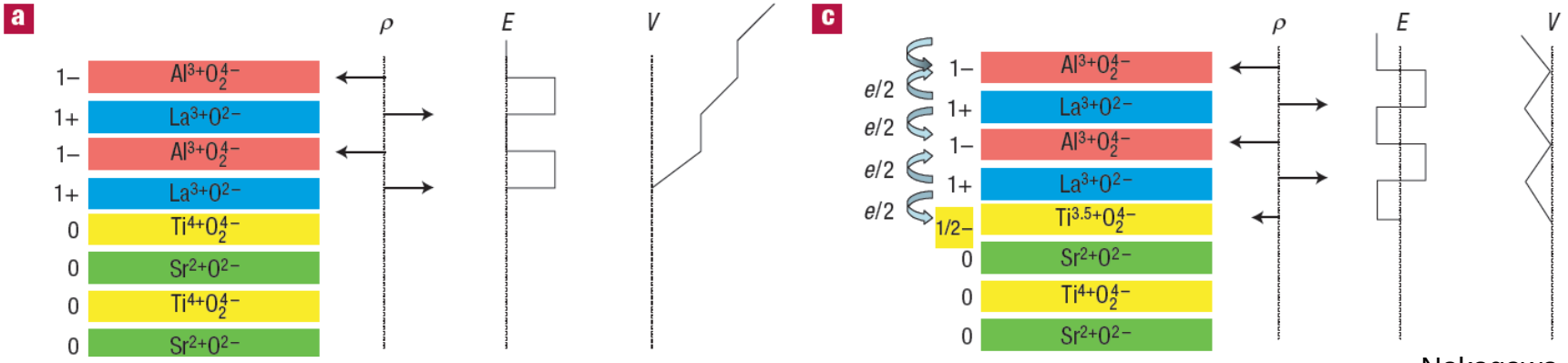

Nakagawa *et al*.

There are a lot of other heterostructures: manganites, nickelates, cuprates, *etc.* and also ferroelectric materials

Recent work on ZnO heterostructures

Quantum Hall effects

- A. Tsukazaki, e*t al*. Quantum Hall effect in polar oxide heterostructures. Science **315**,1388 (2007).

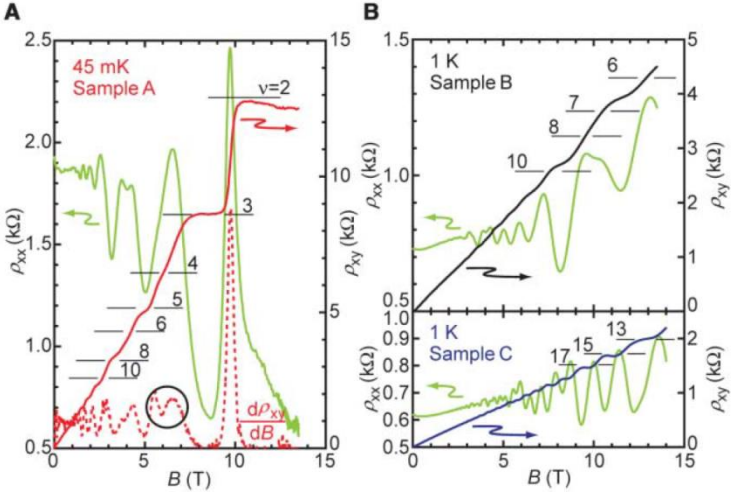

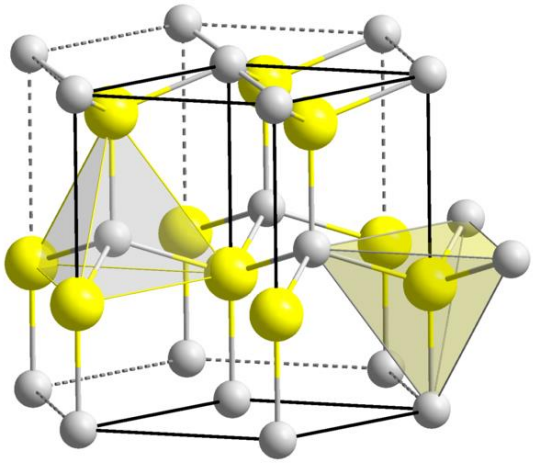

ZnO with wurtzite structure

- A. Tsukazaki, *et al*. Observation of the fractional quantum Hall effect in an oxide, Nature Materials **9**, 889 (2010).

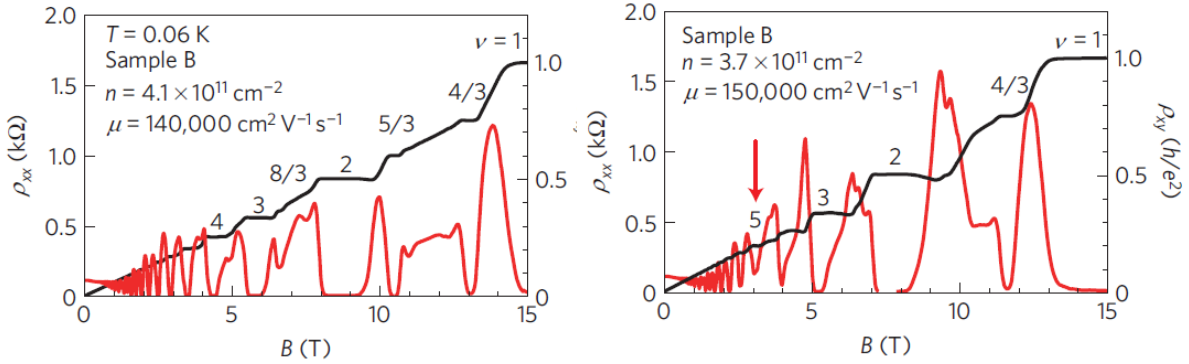

Quality of oxide heterostructures is becoming comparable with that of semiconductors. It is a right moment to explore novel phenomena using complex oxides.

Motivation of our study: Graphene

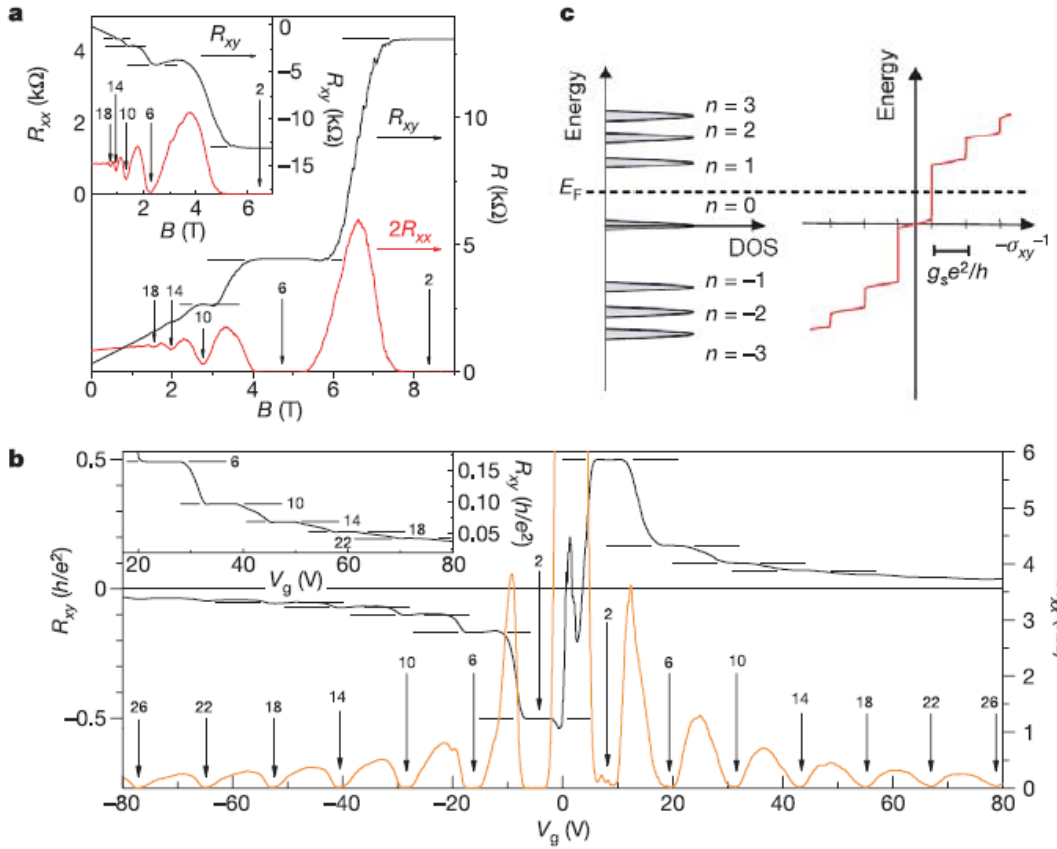

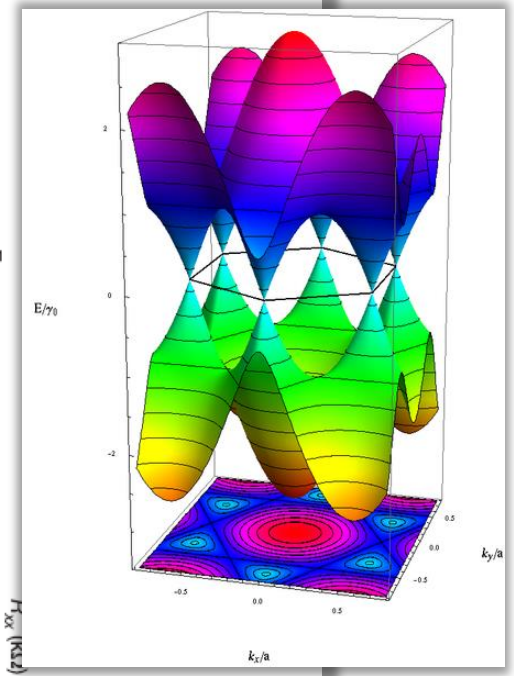

Figure 2 | Quantized magnetoresistance and Hall resistance of a graphene device. **a**, Hall resistance (black) and magnetoresistance (red) measured in the device in Fig. 1 at $T = 30$ mK and $V_g = 15$ V. The vertical arrows and the numbers on them indicate the values of B and the corresponding filling factor ν of the quantum Hall states. The horizontal lines correspond to $h/e^2\nu$ values. The QHE in the electron gas is shown by at least two quantized plateaux in R_{xy}, with vanishing R_{xx} in the corresponding magnetic field regime. The inset shows the QHE for a hole gas at $V_g = -4$ V, measured at 1.6 K. The quantized plateau for filling factor $\nu = 2$ is well defined, and the second and third plateaux with $\nu = 6$ and $\nu = 10$ are also resolved. **b**, Hall resistance (black) and magnetoresistance (orange) as a function of gate voltage at fixed magnetic field $B = 9$ T, measured at 1.6 K. The same convention as in **a** is used here. The upper inset shows a detailed view of high-filling-factor plateaux measured at 30 mK. **c**, A schematic diagram of the Landau level density of states (DOS) and corresponding quantum Hall conductance (σ_{xy}) as a function of energy. Note that, in the quantum Hall states, $\sigma_{xy} = -R_{xy}^{-1}$. The LL index n is shown next to the DOS peak. In our experiment the Fermi energy E_F can be adjusted by the gate voltage, and R_{xy}^{-1} changes by an amount $g_s e^2/h$ as E_F crosses a LL.

Zhang, *et al.*, Nature **438**, 201 (2005).

Quantum Hall effects with massless Dirac fermions

Even more exotic phenomena are anticipated in interacting electron models on honeycomb lattice

Model for a Quantum Hall Effect without Landau Levels: Condensed-Matter Realization of the "Parity Anomaly"

F. D. M. Haldane PRL **61**, 2015 (1988)

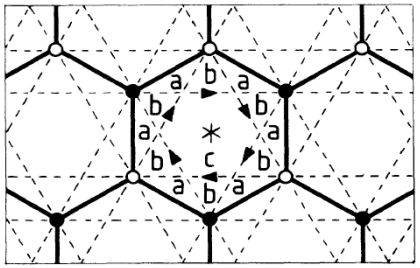

FIG. 1. The honeycomb-net model ("2D graphite") showing nearest-neighbor bonds (solid lines) and second-neighbor bonds (dashed lines). Open and solid points, respectively, mark the *A* and *B* sublattice sites. The Wigner-Seitz unit cell is conveniently centered on the point of sixfold rotation symmetry (marked "*") and is then bounded by the hexagon of nearest-neighbor bonds. Arrows on second-neighbor bonds mark the directions of positive phase hopping in the state with broken time-reversal invariance.

Z_2 Topological Order and the Quantum Spin Hall Effect

C. L. Kane and E. J. Mele PRL **95**, 146802 (2005)

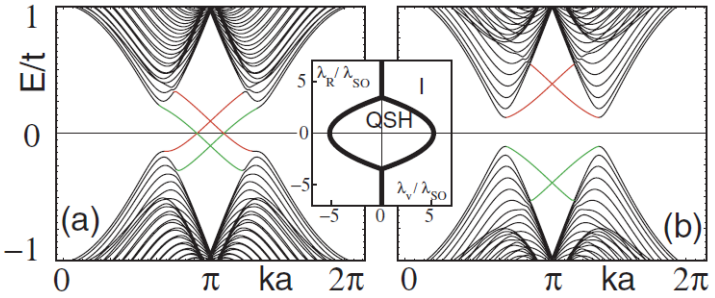

FIG. 1 (color online). Energy bands for a one-dimensional "zigzag" strip in the (a) QSH phase $\lambda_v = 0.1t$ and (b) the insulating phase $\lambda_v = 0.4t$. In both cases $\lambda_{SO} = .06t$ and $\lambda_R = .05t$. The edge states on a given edge cross at $ka = \pi$. The inset shows the phase diagram as a function of λ_v and λ_R for $0 < \lambda_{SO} \ll t$.

Topological Mott Insulators

S. Raghu,[1] Xiao-Liang Qi,[1] C. Honerkamp,[2] and Shou-Cheng Zhang[1] PRL**100**, 156401 (2008)

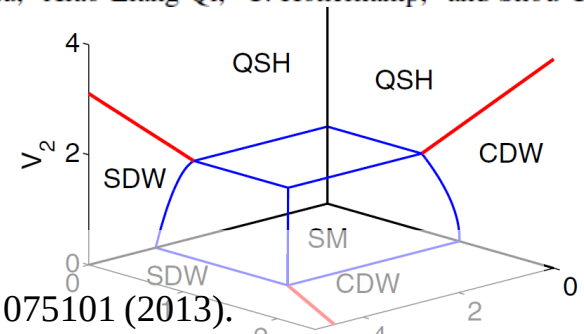

FIG. 3 (color online). Complete mean-field phase diagram for the spinful model. The transitions from the semimetal (SM) to the insulating phases are continuous, whereas transitions between any two insulating phases are first order.

Still under debate
Jia, *et al*., PRB **88**, 075101 (2013).
Daghofer and Hohenadler, PRB **89**, 035103 (2014).
Scherer, Scherer, and Honerkamp, arXiv:1507.08123.

Leading to one of the hottest areas in condensed matter physics: Topological insulators

Question: Can we explore such novel physics using complex (perovskite) oxides?

Merit using perovskite oxides

- In principle, electron-electron interactions and spin-orbit coupling can be controlled.
- Different exotic phases can be combined in heterostructures, such as SC, magnetism & Mott insulators.

Outline

- **Oxide heterostructures**
- **Motivation**
- **Designing novel quantum states**
  - **Quantum spin Hall effects**
  - **Correlation-induced Mott transition**
  - **Approach from Mott insulators**

Poor man's strategy

1. Mimic graphene (create honeycomb lattice)
2. Locate the Fermi level at Dirac points
3. Spin-orbit coupling would create 2D TI states

How can we realize honeycomb lattice?

Perovskite structure from the [001] direction

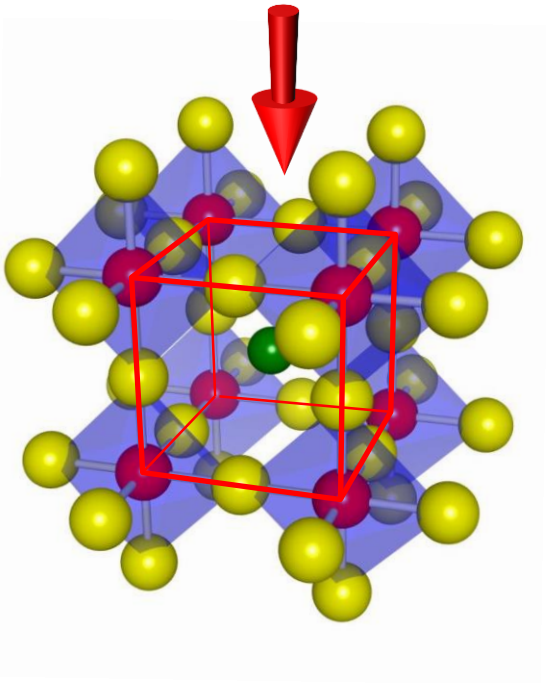

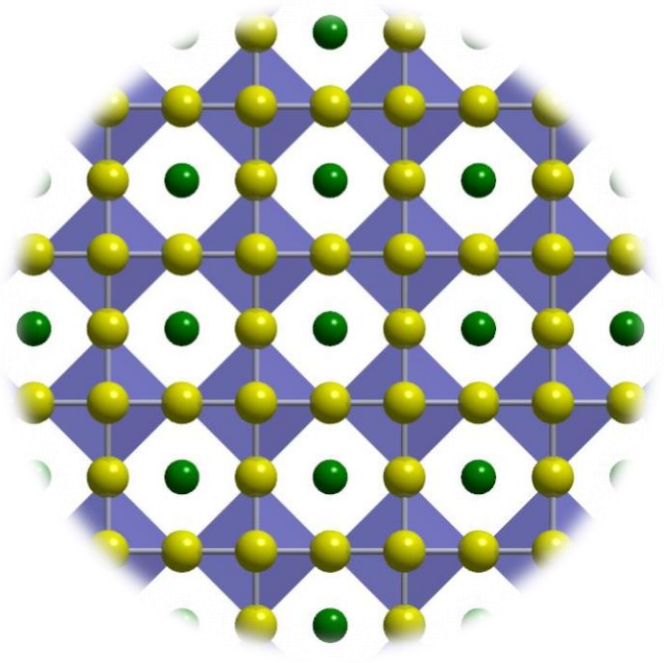

Square lattice

Poor man's strategy

1. Mimic graphene (create honeycomb lattice)
2. Locate the Fermi level at Dirac points
3. Spin-orbit coupling would create 2D TI states

How can we realize honeycomb lattice?

Perovskite structure from the [111] direction

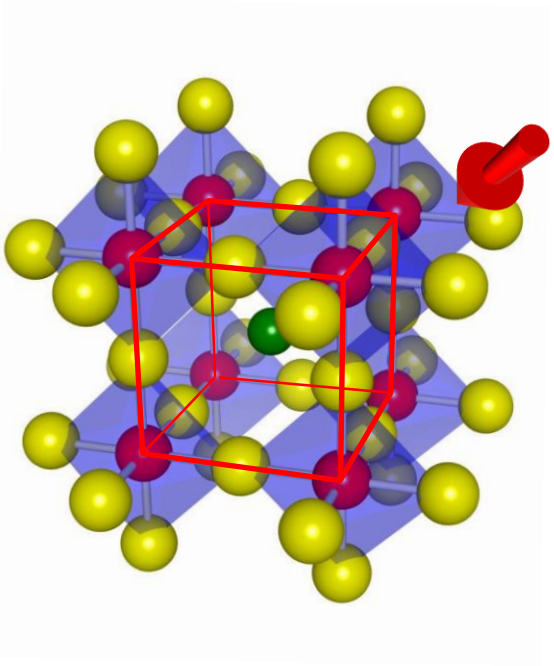

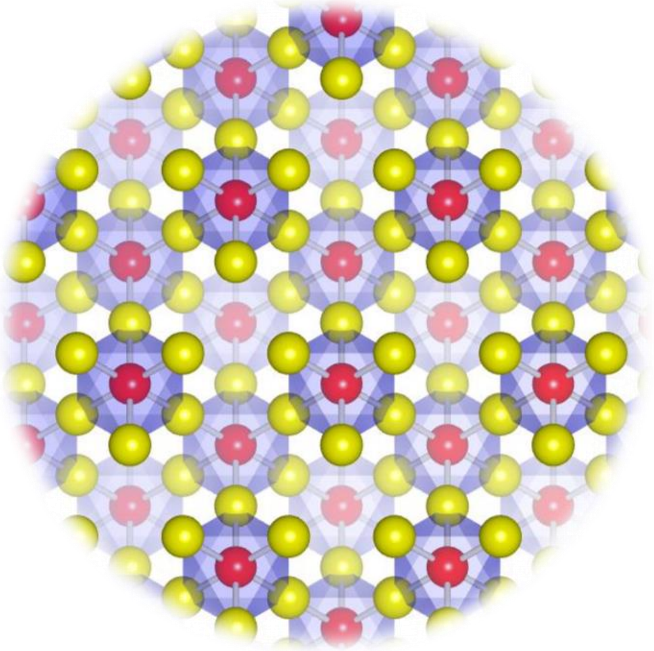

Trigonal symmetry

Poor man's strategy

1. Mimic graphene (create honeycomb lattice)
2. Locate the Fermi level at Dirac points
3. Spin-orbit coupling would create 2D TI states

How can we realize honeycomb lattice?

Perovskite structure from the [111] direction confined in "bilayer"

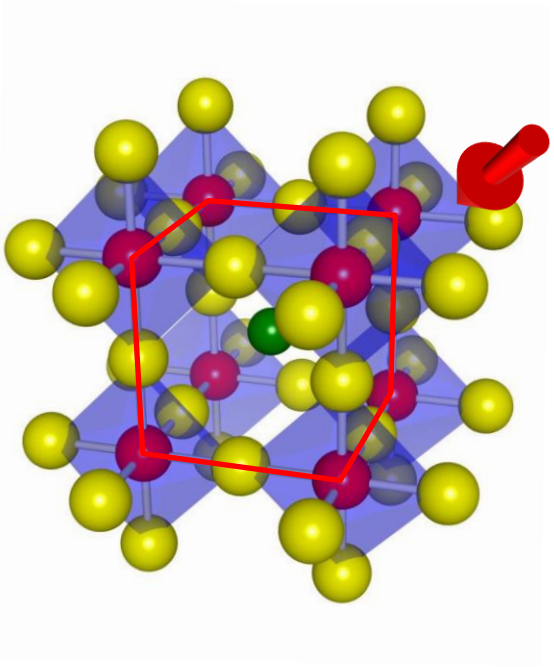

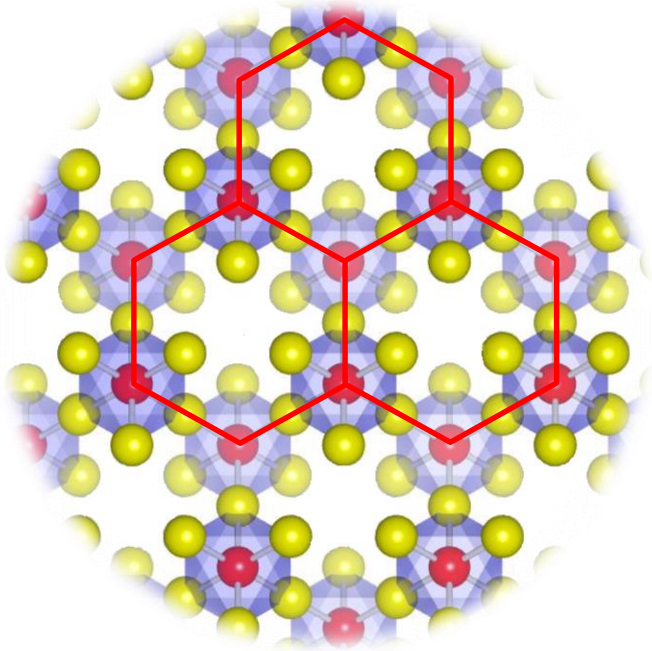

"Buckled" honeycomb lattice

How to stabilize (111) bilayer of perovskite ABO_3

Pulsed Laser Deposition or molecular beam “hetero” epitaxy

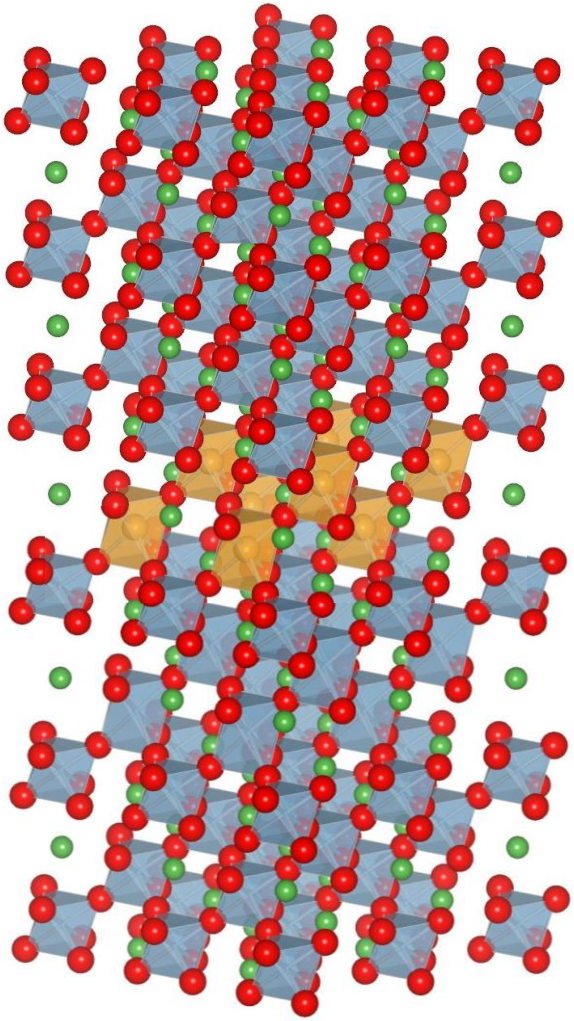

$AB'O_3$ capping layers

← 2nd ABO_3 block
← 1st ABO_3 block
} ABO_3 (111) bilayer

← AO_3 layer
← B' layer
} $AB'O_3$ unit

$AB'O_3$ substrate with [111] surface

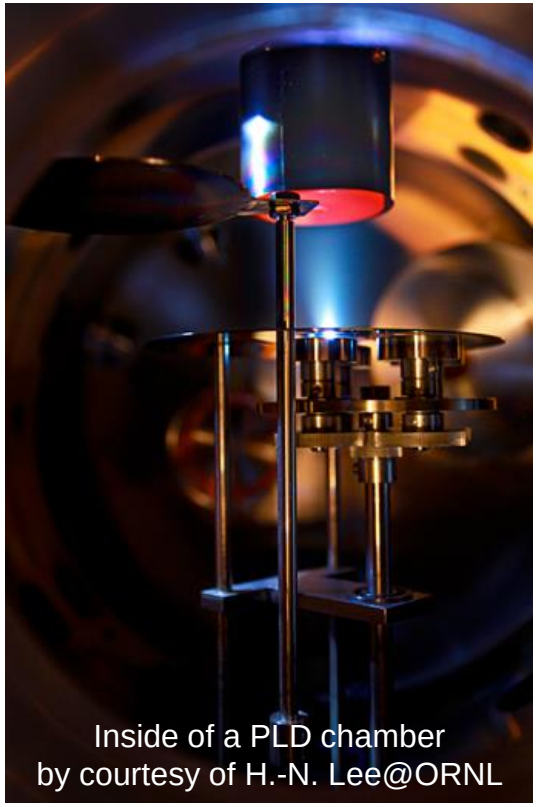

Inside of a PLD chamber
by courtesy of H.-N. Lee@ORNL

Tight binding models

t_{2g} systems

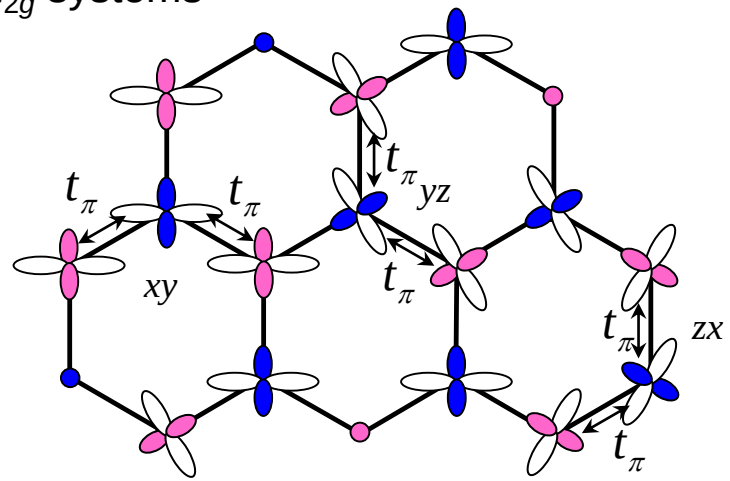

e_g systems

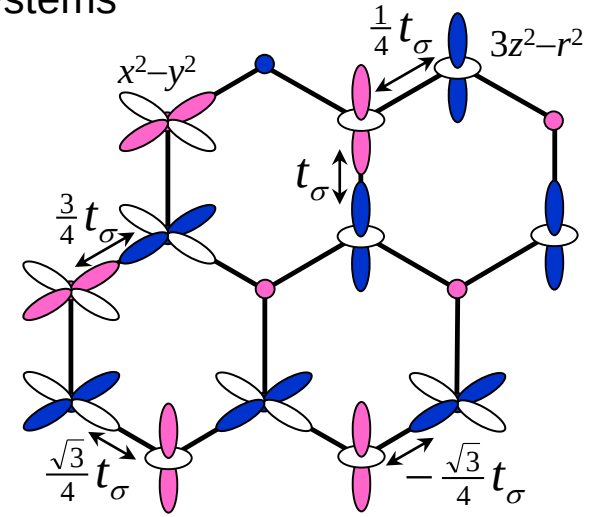

Spin-orbit coupling $\lambda\vec{l}_i\cdot\vec{s}_i \Rightarrow -\lambda\vec{l}_i\cdot\vec{s}_i$

l=2 l=1

projected on the t_{2g} multiplet

$$\sum_{\tau\notin e_g}\frac{\langle l|\lambda\vec{l}_i\cdot\vec{s}_i|\tau\rangle\langle\tau|\lambda\vec{l}_i\cdot\vec{s}_i|m\rangle}{E_{e_g}-E_\tau}=-\tilde{\lambda}\sum_{\varepsilon\varepsilon'\sigma}c^\dagger_{i\varepsilon\sigma}\tau^y_{\varepsilon\varepsilon'}\tau^z_{\sigma\sigma}c_{i\varepsilon'\sigma}$$

Vallin, PRB **2,** 2390 (1970).
Chen, Balents, Schnyder, PRL **102,** 096406 (2009).

Trigonal crystal field $\Delta\sum_{\substack{\alpha\neq\beta\\ \in t2g}}\alpha_i^\dagger\beta_j$

Single-particle energy level

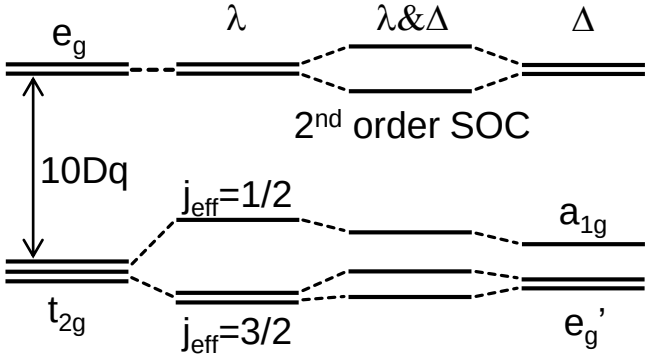

Tight binding dispersion

t_{2g} systems

Possible candidates for 2D TIs:
t_{2g}^1, t_{2g}^2, t_{2g}^4, t_{2g}^5

e_g systems

Possible candidates for 2D TIs:
e_g^1, e_g^2, e_g^3

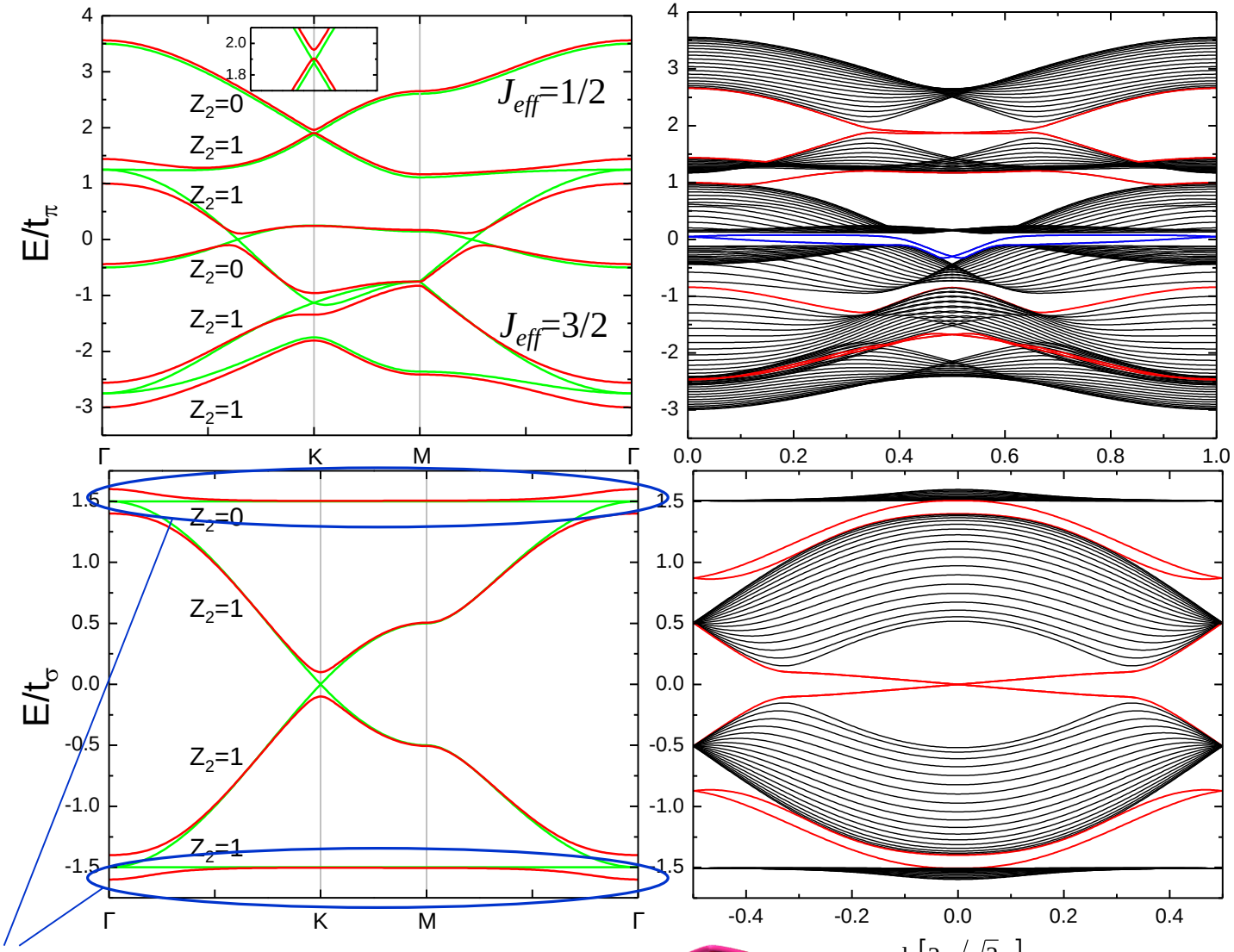

Flat bands/quadratic band crossing w/o SOC
Even more exotic phenomena?

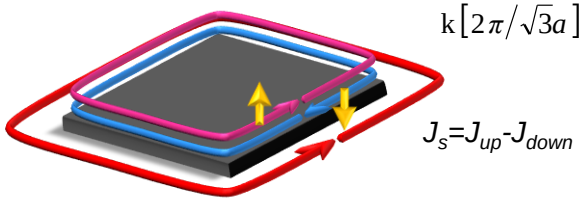

Materials search

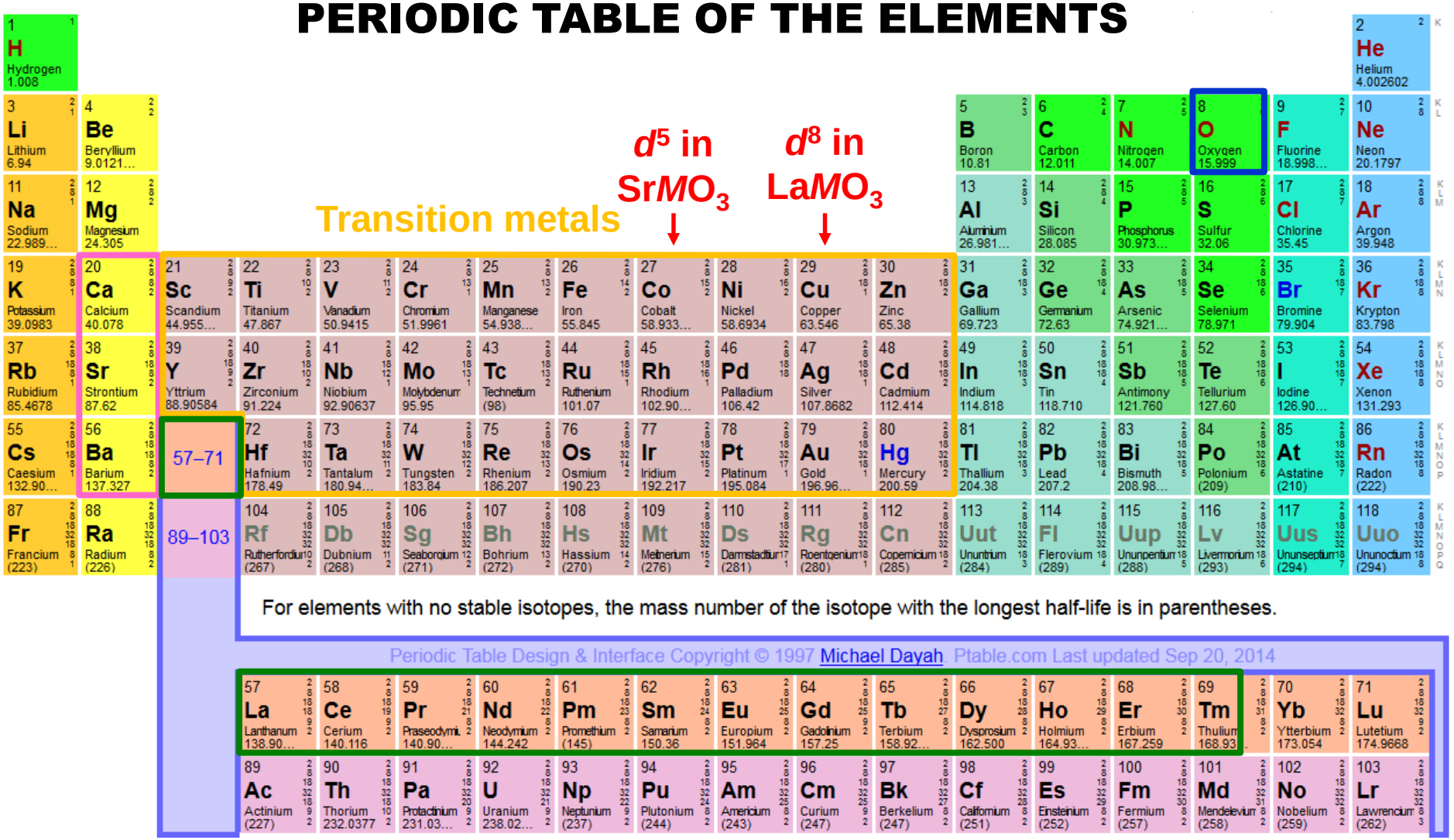

Candidate materials

	Configuration	Bulk	Superlattice
$LaReO_3$	t_{2g}^4	—	—
$LaRuO_3$	t_{2g}^5	Metallic[27]	—
$SrRhO_3$	t_{2g}^5	Metallic[28]	(Ref. 29)
$SrIrO_3$	t_{2g}^5	Metallic[30,31]	Metallic[32]
$LaOsO_3$	t_{2g}^5	—	—
$LaAgO_3$	e_g^2	Metallic (band calculation)[33]	—
$LaAuO_3$	e_g^2	Not perovskite[34,35]	—

References

27. Sugiyama, T. & Tsuda, N. Electrical and magnetic properties of $Ca_{1-x}La_xRuO_3$. *J. Phys. Soc. Jpn.* **68,** 3980–3987 (1999).
28. Yamaura, K. & Takayama-Muromachi, E. Enhanced paramagnetism of the 4*d* itinerant electrons in the rhodium oxide perovskite $SrRhO_3$. *Phys. Rev. B* **64,** 224424 (2001).
29. Desu, S. B., Yoo, I. K., Kwok, C. K., & Vijay, D. P. Multilayer electrodes for ferroelectric devices European Patent EP0636271 (1995).
30. Cao, G. *et al.* Non-Fermi-liquid behavior in nearly ferromagnetic $SrIrO_3$ single crystals. *Phys. Rev. B* **76,** 100402(R) (2007).
31. Moon, S. J. *et al.* Dimensionality-controlled insulator-metal transition and correlated metallic state in 5*d* transition metal oxides $Sr_{n+1}Ir_nO_{3n+1}$ (n=1,2, and ∞). *Phys. Rev. Lett.* **101,** 226402 (2008).
32. Sumi, A. *et al.* MOCVD growth of epitaxial $SrIrO_3$ films on (111)$SrTiO_3$ substrates. *Thin Solid Films* **486,** 182–185 (2005).
33. Bacalis, N. C. Band structure and electron-phonon interaction of $LaAgO_3$. *J. Superconductivity* **1,** 175–180 (1988).
34. Guruswany, V., Keillor, P., Campbell, G. L. & Bockris, J.O'M. The photoelectrochemical response of the lanthanides of chromium, rhodium, vanadium and gold on a titanium base. *Solar Energy Materials* **4,** 11–30 (1980).
35. Ralle, M. & Jansen, M. Synthesis and crystal structure determination of $LaAuO_3$. *J. Solid State Chem.* **105,** 378–384 (1993).

DFT results

Tight-binding modeling: $t_{2g}^{1,2,4,5}$ and $e_g^{1,2,3}$ systems could become 2D TIs.

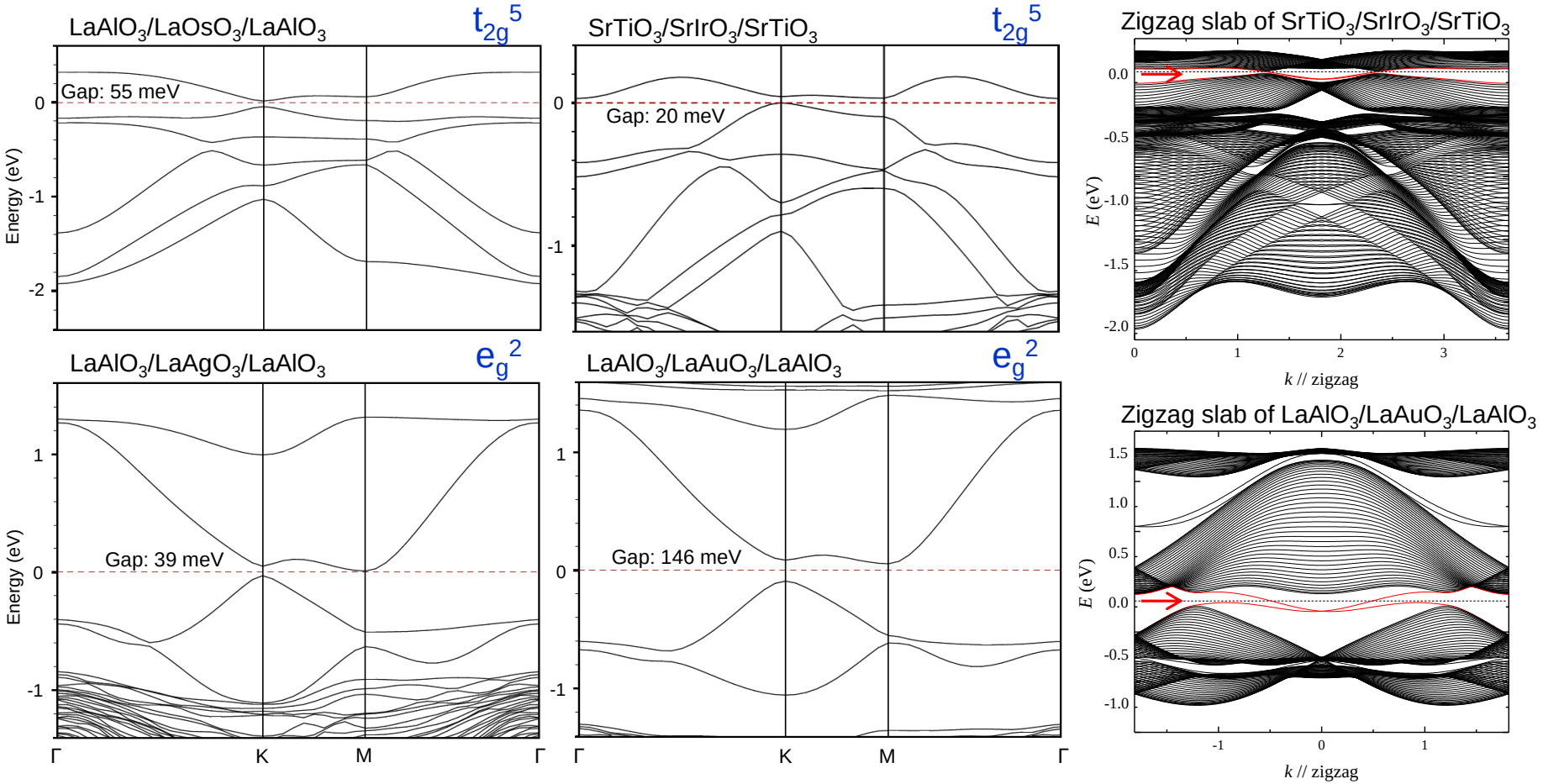

DFT confirmation: (111) bilayers of $LaOsO_3$, $SrIrO_3$, $LaAgO_3$, and $LaAuO_3$ are 2D TIs.

$LaReO_3$, $LaRuO_3$ and $SrRhO_3$ are topological semimetals, and $LaCuO_3$ is an AF trivial insulator.

How about correlation effects??

Outline

- **Oxide heterostructures**
- **Motivation**
- **Designing novel quantum states**
  - **Quantum spin Hall effects**
  - **Correlation-induced Mott transition**
  - **Approach from Mott insulators**

Correlation effects

1. Symmetry breaking (spin, orbital, charge, etc)

2. Mott “metal”-insulator transition

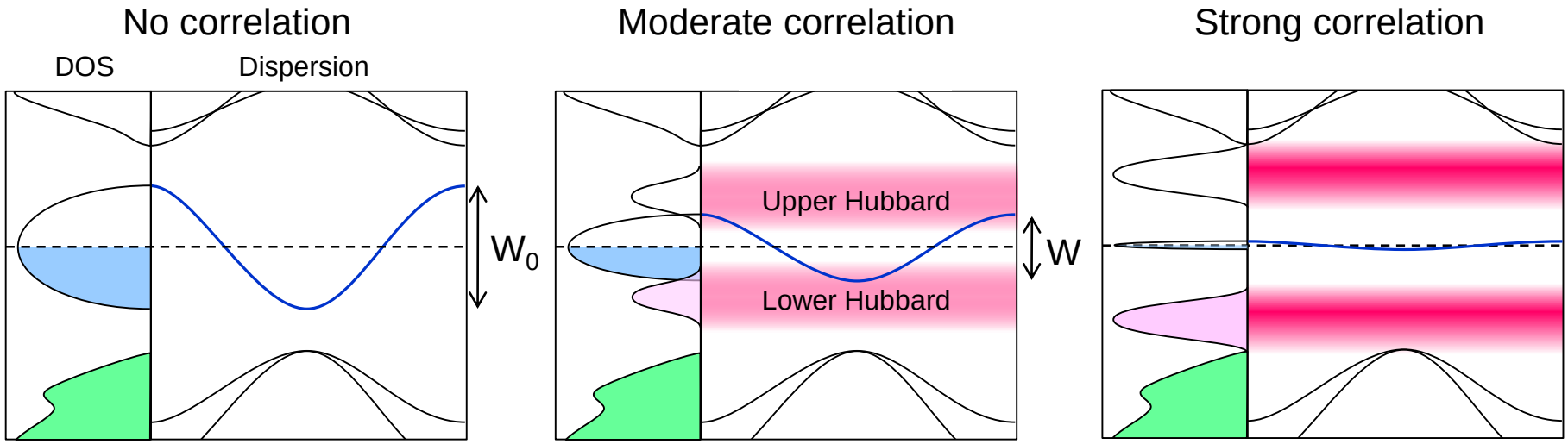

W_0: bare band width

W: renormalized band width
$W/W_0 \sim Z$: quasiparticle weight
1/Z: mass enhancement

$Z \Rightarrow 0$
Infinite effective mass
Mott insulator

Dynamical mean-field theory [Georges (previous talk), Kotliar]:
A methodology that can deal with correlation effects beyond a static mean-field approximation

Static mean-field theory vs. dynamical mean-field theory

A. Georges, et al. RMP **68**, 13 (1996).

Static mean-field theory

Lattice model

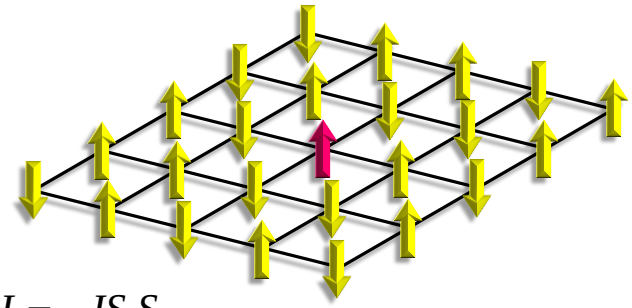

$$H = -JS_iS_j$$

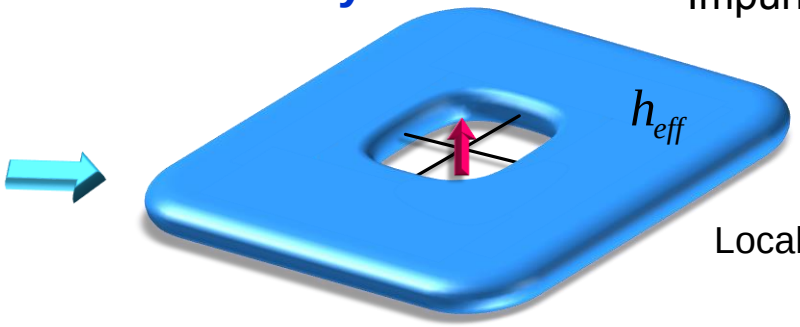

"Impurity" model

$$H_{eff} = -h_{eff}S_0$$

$$h_{eff} = zJ\langle S_i\rangle$$

Local observable

$$\langle S_0\rangle$$

Self consistency

$$\langle S_i\rangle = \langle S_0\rangle$$

Dynamical mean-field theory

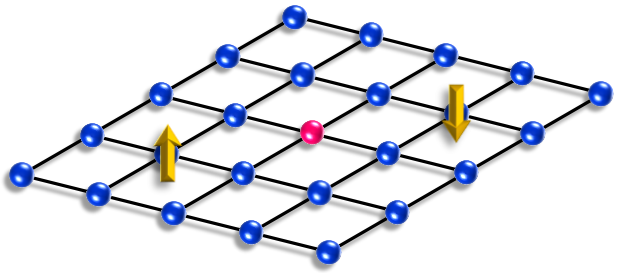

$$H = t_{ij}^{\alpha\beta} d_{i\alpha}^{\dagger} d_{j\beta} + H_{\text{int}}$$

$$= \varepsilon_k^{\alpha\beta} d_{k\alpha}^{\dagger} d_{k\beta} + H_{\text{int}}$$

$$G_{\alpha\beta}^{loc}(i\omega_n) = \int \frac{d^d k}{(2\pi)^d} \left[(i\omega_n + \mu)\hat{1} - \hat{\varepsilon}_k - \hat{\Sigma}(i\omega_n) \right]^{-1}_{\alpha\beta}$$

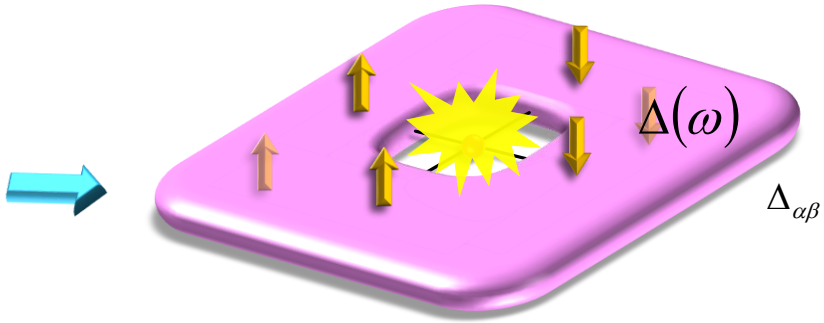

$$\Delta_{\alpha\beta}(\omega) = \sum_k \frac{V_{k\alpha}^* V_{k\beta}}{\omega - \tilde{\varepsilon}_k}$$

$$H_{eff} = t_{00}^{\alpha\beta} d_{0\alpha}^{\dagger} d_{0\beta} + H_{\text{int},0} + \sum_k \left(\tilde{\varepsilon}_k c_k^{\dagger} c_k + V_{k\alpha} c_k^{\dagger} d_{0\alpha} + h.c. \right)$$

Local observable: electron Green's function

$$G_{\alpha\beta}(i\omega_n) = \left[(i\omega_n + \mu)\hat{1} - \hat{t}_{00} - \hat{\Sigma}(i\omega_n) - \hat{\Delta}(i\omega_n) \right]^{-1}_{\alpha\beta}$$

Self consistency $G_{\alpha\beta}^{loc}(i\omega_n) = G_{\alpha\beta}(i\omega_n)$

* Finite temperature exact diagonalization impurity solver (work on other systems in progress using CT-QMC)

M. Caffarel and W. Krauth, PRL **72**, 1545 (1994).
C. A. Perroni, *et al*. PRB **75**, 045125 (2007).
M. Capone, *et al*. PRB **76**, 245116 (2007).

Comparison between DFT (Wannier) band structure and DMFT spectral function

DFT (Wannier) band structure **Typical DMFT spectral function, U=2, J=0.2 eV**

$SrIrO_3$
(111) bilayer

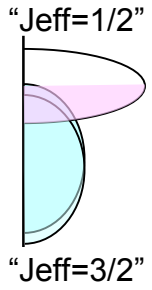

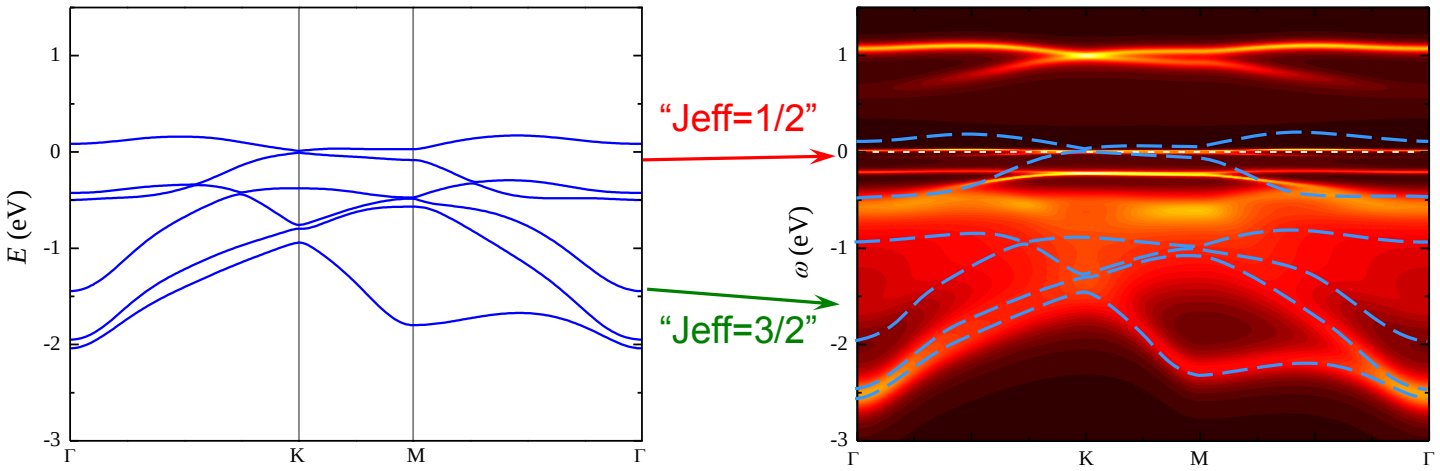

$LaAuO_3$
(111) bilayer

Two Kramers states

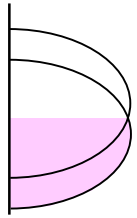

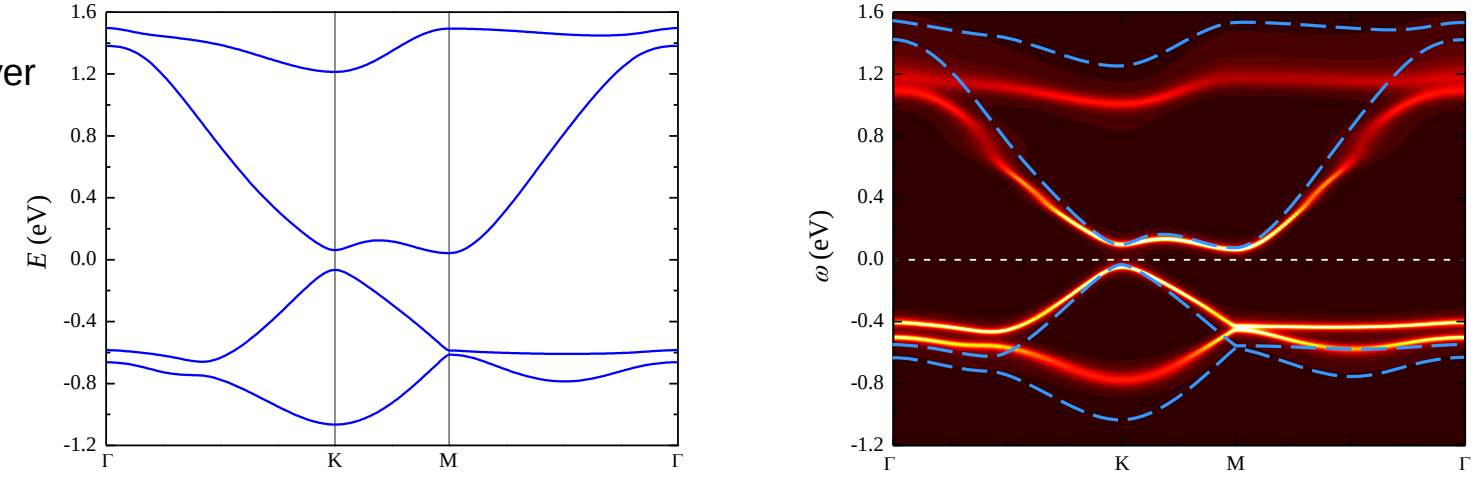

- Correlation effects are strong in $SrIrO_3$ bilayer, especially near the Fermi-level regime with strong "J_{eff}=1/2" character (the separation between J_{eff}=1/2 and J_{eff}=3/2 is not complete).
- Moderate band renormalization in $LaAuO_3$ bilayer.

DMFT results: Mott metal-insulator transition without magnetic ordering

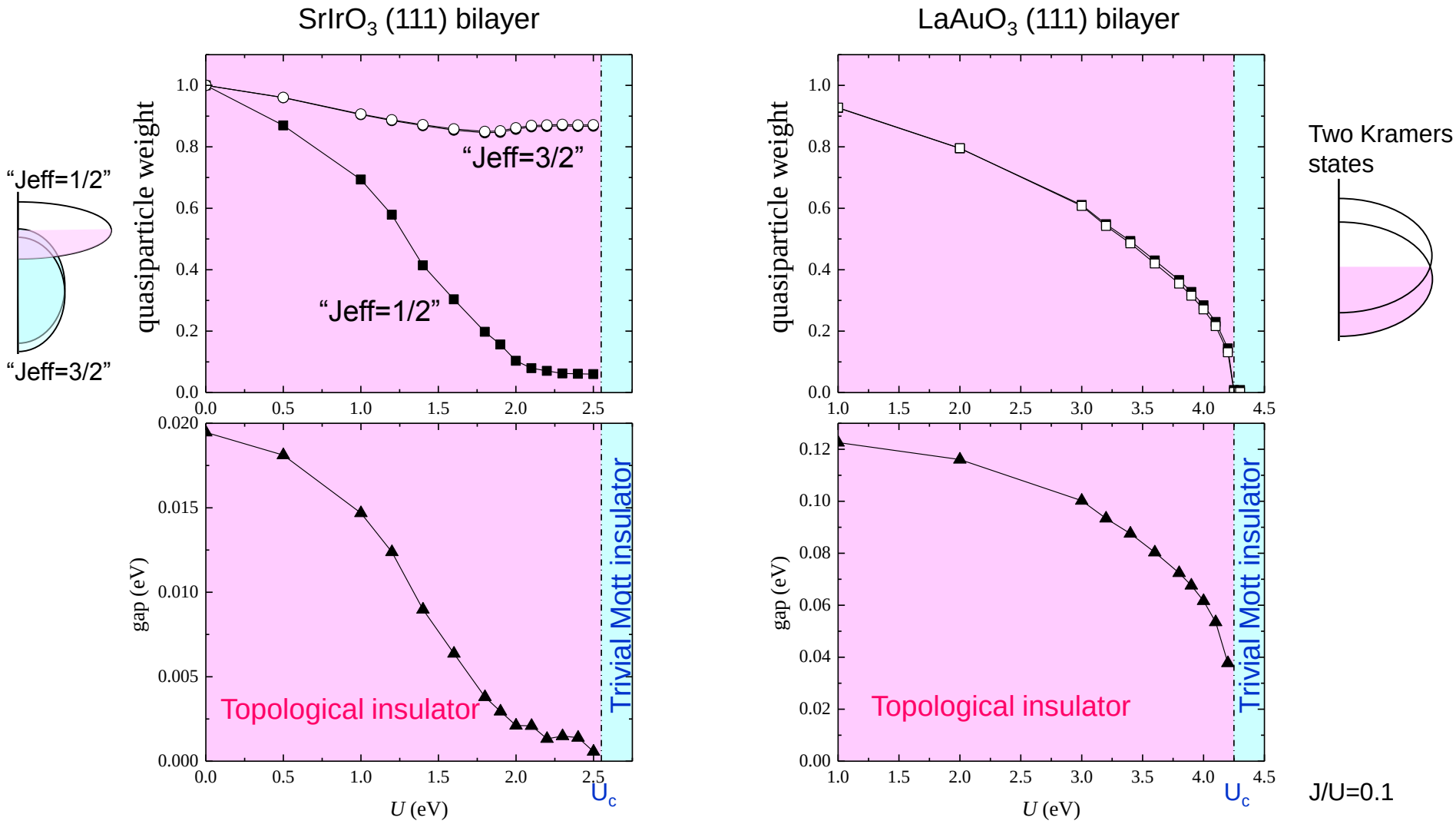

- At the metal-insulator transition of $SrIrO_3$ bilayer, only "J_{eff}=1/2" states have strong mass renormalization: *orbital-selective topological Mott transition*.
- For $LaAuO_3$ bilayer, two Kramers states show nearly identical mass renormalization.

DMFT results: Transition to Néel antiferromagentic phases

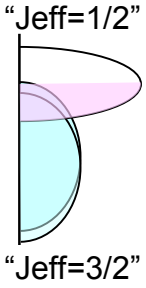

$SrIrO_3$ (111) bilayer

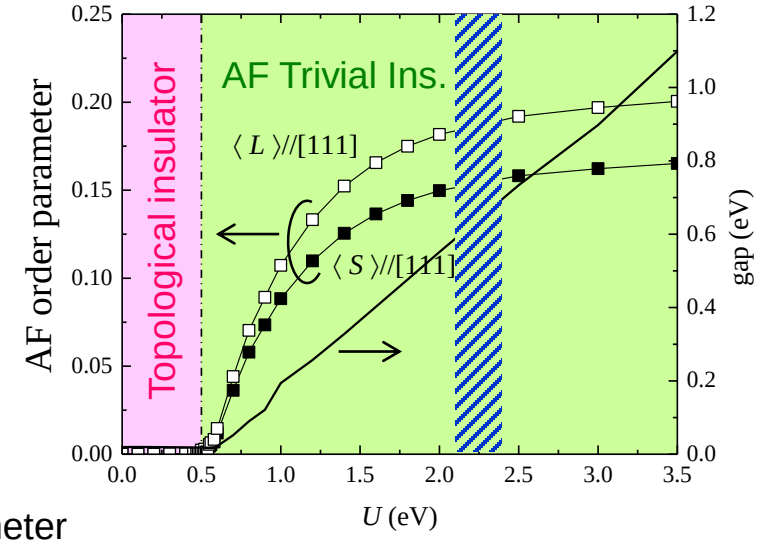

Parameter estimation by cRPA:

U=2.232, J=0.202 eV
[Arita *et al*., PRL, **108**, 086403 (2012)]

$LaAuO_3$ (111) bilayer

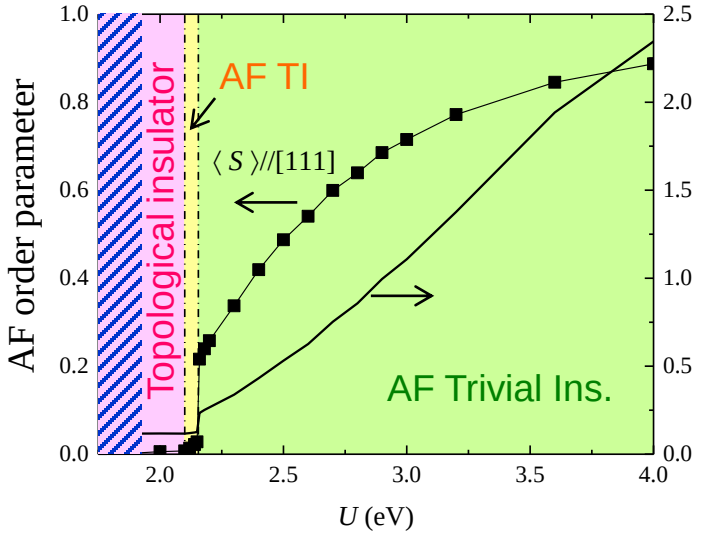

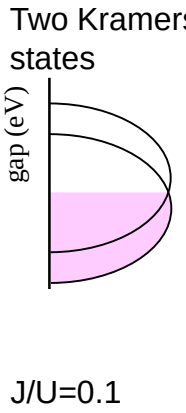

U=1.80, J=0.225 eV
[present work by Nomura, Arita]

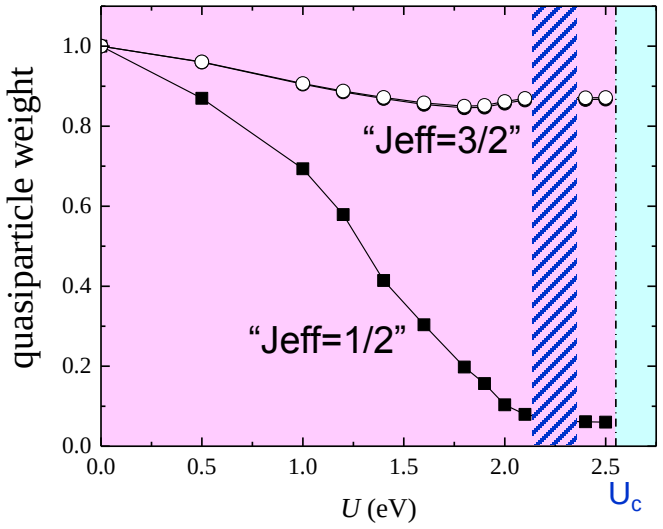

- $LaAuO_3$ (111) bilayer is in a TI regime.
- The critical U for an AF ordering is small ~0.5eV for $SrIrO_3$ (111) bilayer ⇐ narrow band width of "J_{eff}=1/2 state".
- $SrIrO_3$ (111) bilayer is an AF trivial insulator.
- AF ordering is essential for the insulating nature, similar to Sr_2IrO_4 [Arita, Imada et al., PRL **108**, 086403 (2012), Zhang, Haule, Vanderbilt, PRL **111**, 246402 (2013)].

DMFT results: Transition to Néel antiferromagentic phases

$SrIrO_3$ (111) bilayer

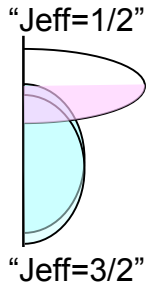

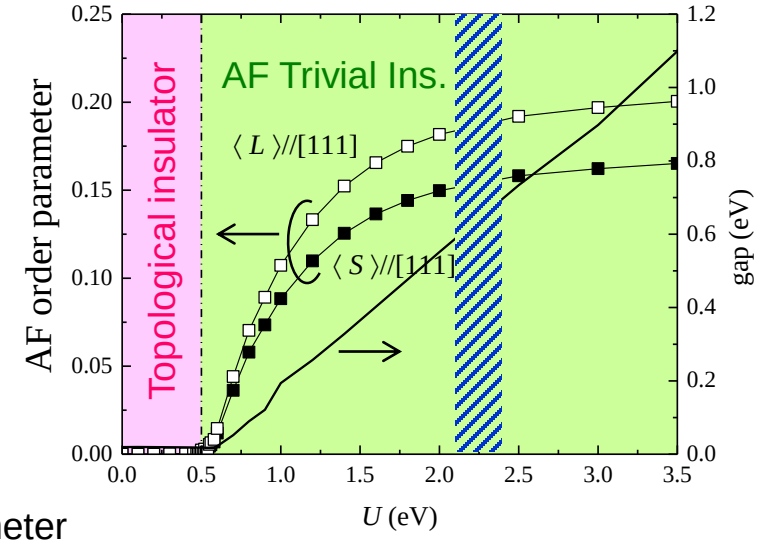

$LaAuO_3$ (111) bilayer

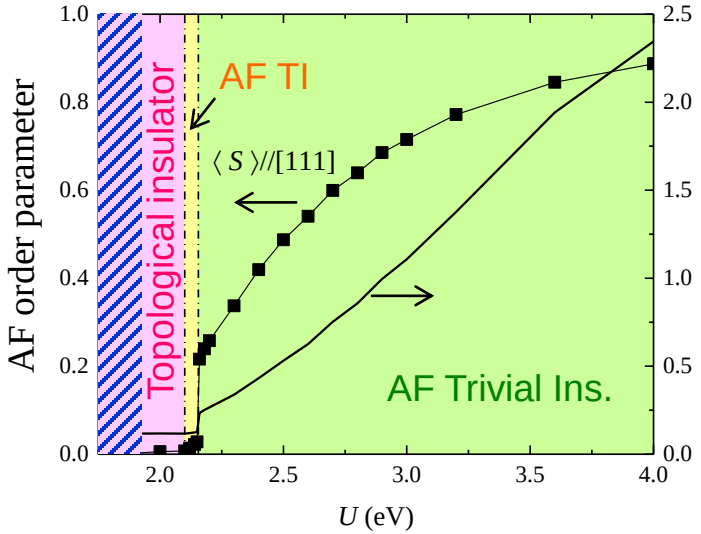

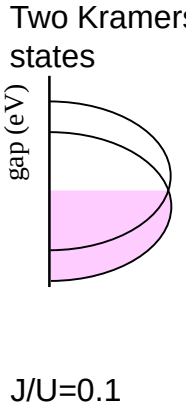

Parameter estimation by cRPA:

U=2.232, J=0.202 eV
[Arita *et al.*, PRL, **108**, 086403 (2012)]

U=1.80, J=0.225 eV
[present work by Nomura, Arita]

Edge spectra:

No gapless edge mode →

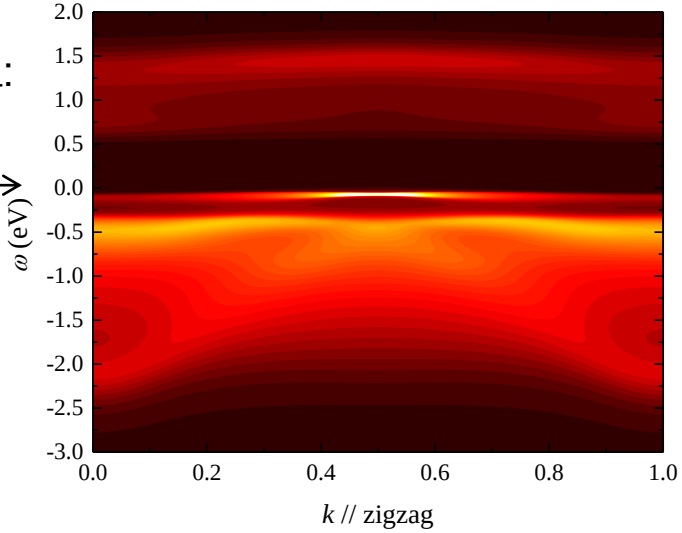

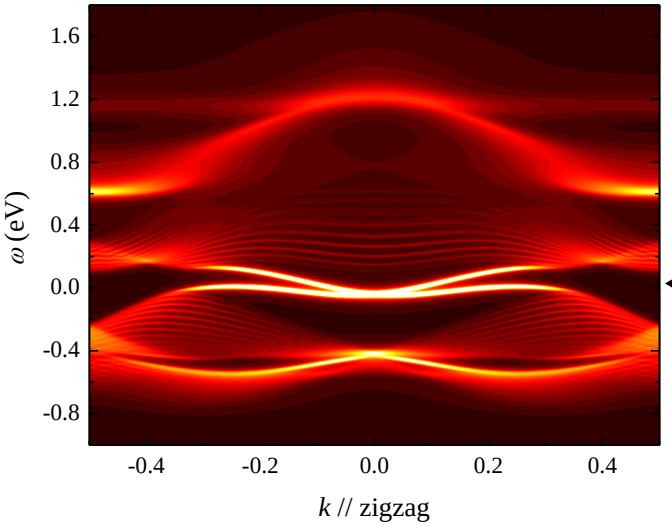

← Gapless edge modes

- $SrIrO_3$ (111) bilayer is an AF trivial insulator, while $LaAuO_3$ (111) bilayer is a TI.

Outline

- **Oxide heterostructures**
- **Motivation**
- **Designing novel quantum states**
  - **Quantum spin Hall effects**
  - **Correlation-induced Mott transition**
  - **Approach from Mott insulators**

Generic phase diagram of integer-filling correlated systems

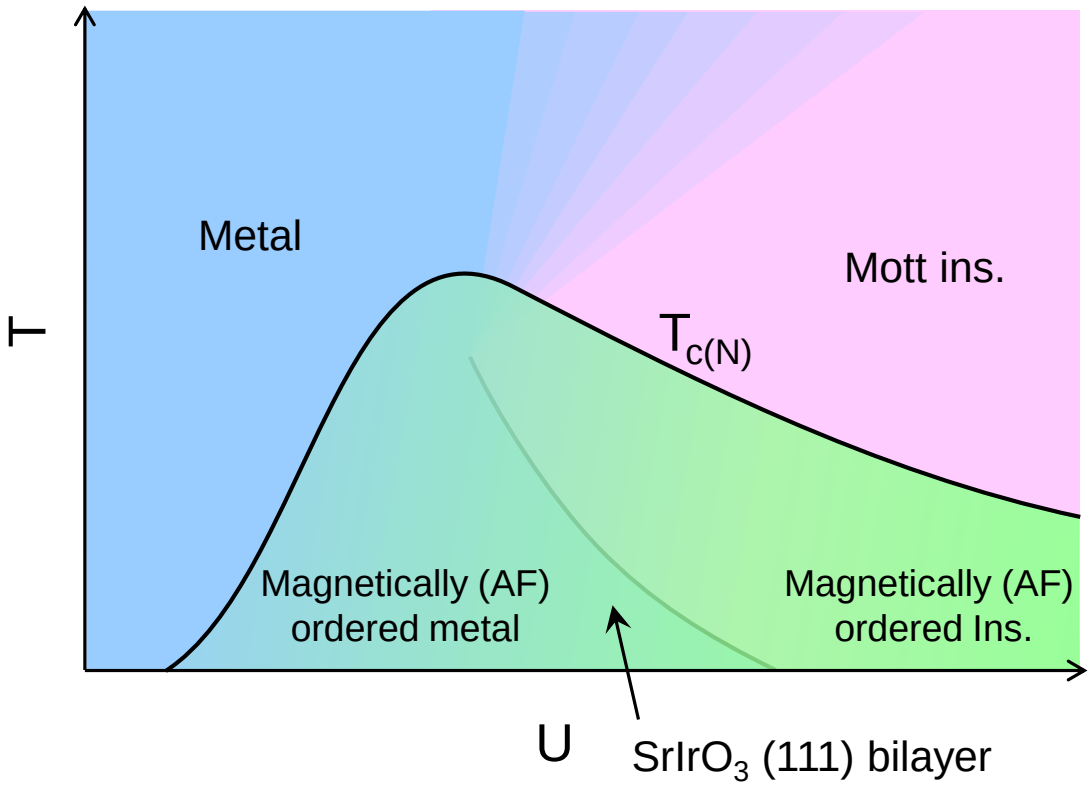

- AF insulator phases at small U (Slater AF insulator) and large U (Mott insulator with AF ordering) are adiabatically connected.
- $SrIrO_3$ (111) bilayer is indeed very strongly correlated, and approach from the Mott insulator side may be also valid to discuss magnetic ground states, excitations, and doping effects.

What is the effect of strong correlations in Mott insulating states with the strong spin-orbit coupling as in (111) bilayer of $SrIrO_3$?

Low-energy Hamiltonians for such systems (t_{2g}^5 electronic systems) could be described in terms of "J_{eff}=1/2".

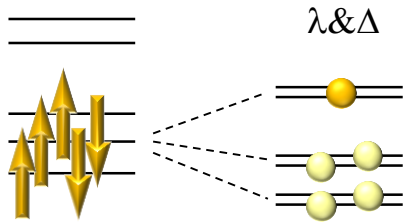

t_{2g}^5

$SrTiO_3/SrIrO_3/SrTiO_3$

Novel phenomena???

Models

Hopping

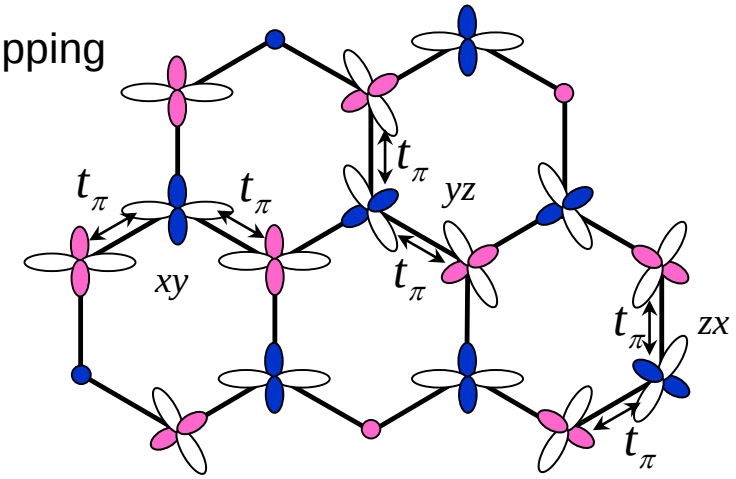

Rotationally symmetric Coulomb interactions

$$^3T_2 : U-3J : |\alpha_\sigma\beta_\sigma\rangle, \frac{1}{\sqrt{2}}\left\{|\alpha_\sigma\beta_{\bar\sigma}\rangle + |\alpha_{\bar\sigma}\beta_\sigma\rangle\right\}$$

$$^3T_1 : U-J : \frac{1}{\sqrt{2}}\left\{|\alpha_\sigma\beta_{\bar\sigma}\rangle - |\alpha_{\bar\sigma}\beta_\sigma\rangle\right\}$$

$$^1T_2 : U-J : \begin{cases} \frac{1}{\sqrt{2}}\left\{|a_\uparrow a_\downarrow\rangle - |b_\uparrow b_\downarrow\rangle\right\} \\ \frac{1}{\sqrt{6}}\left\{|a_\uparrow a_\downarrow\rangle + |b_\uparrow b_\downarrow\rangle - 2|c_\uparrow c_\downarrow\rangle\right\} \end{cases}$$

$$^1T_1 : U+2J : \frac{1}{\sqrt{3}}\left\{|a_\uparrow a_\downarrow\rangle + |b_\uparrow b_\downarrow\rangle + |c_\uparrow c_\downarrow\rangle\right\}$$

For the minimum excitation energy become positive, $U>3J$

Spin-orbit coupling $-\lambda\vec{l}_i\cdot\vec{s}_i$

~~Trigonal crystal field $\Delta\sum_{\substack{\alpha\neq\beta \\ \in t2g}}\alpha_i^\dagger\beta_j$~~

DFT estimates:
λ~0.1 eV
Δ~0.01 eV

Derivation of effective interactions

Second-order perturbation with respect to hopping term
c.f. deriving Heisenberg interaction from single-band Hubbard model

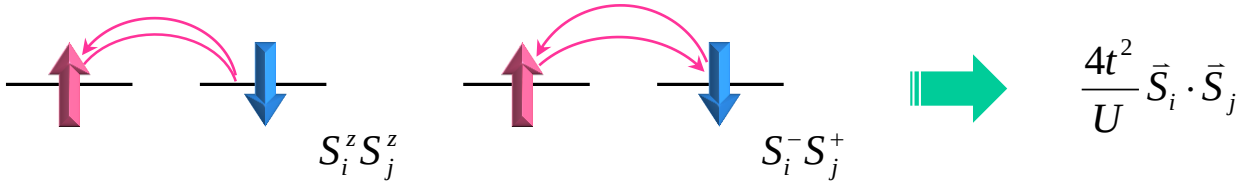

Effective Hamiltonian

- t_{2g}^5 AFM Kitaev-AFM Heisenberg model

$$H = J_K \sum_{\langle ij \rangle} S_i^\gamma S_j^\gamma + J_H \sum_{\langle ij \rangle} \vec{S}_i \cdot \vec{S}_j$$

Leading terms

$$J_K = \frac{4t_\pi^2}{9(U-3J)} \qquad J_H = \frac{8t_\pi^2}{9(U-3J)}$$

Jackeli and Khaliullin, PRL **101**, 216804 (2008)

Kitaev model
(1st term)

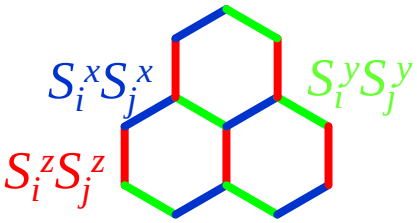

"gapless Z_2 spin liquid"

Kitaev, Ann. Phys. **321**, 2 (2006).

Exact diagonalization results on 24-site clusters

AFM Kitaev-AFM Heisenberg

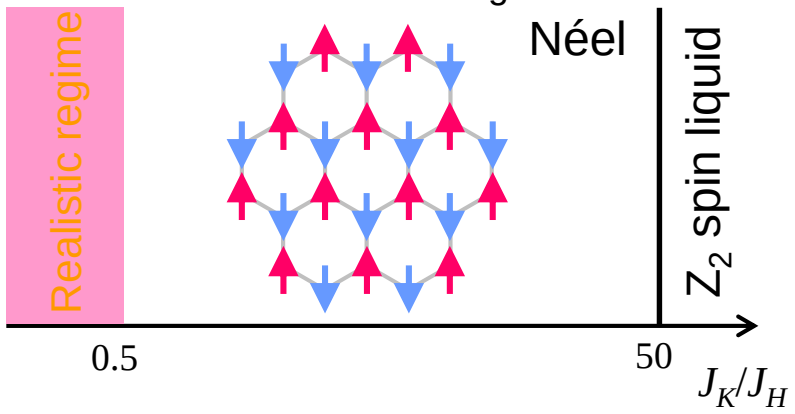

FM Kitaev-AFM Heisenberg

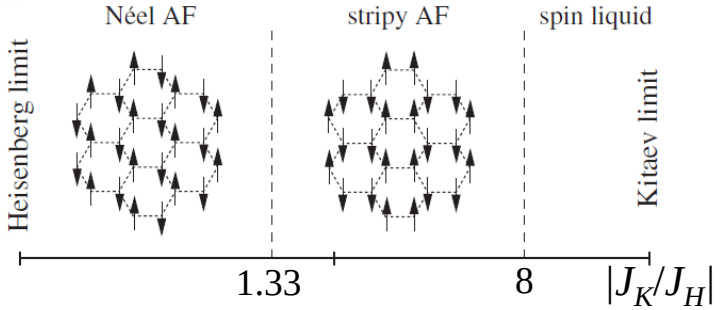

Chaloupka *et al*., PRL **105**, 027204 (2010).

- **Néel AF state is indeed the ground state, consistent with our DMFT results.**
- **A novel spin liquid phase is too far…**

How about carrier doping??

Let's try slave boson mean field calculation

Lee, Nagaosa, and Wen, RMP **78**, 17 (2006).

SU(2) slave-boson mean-field phase diagram

t_{2g}^5 AFM Kitaev-AFM Heisenberg model

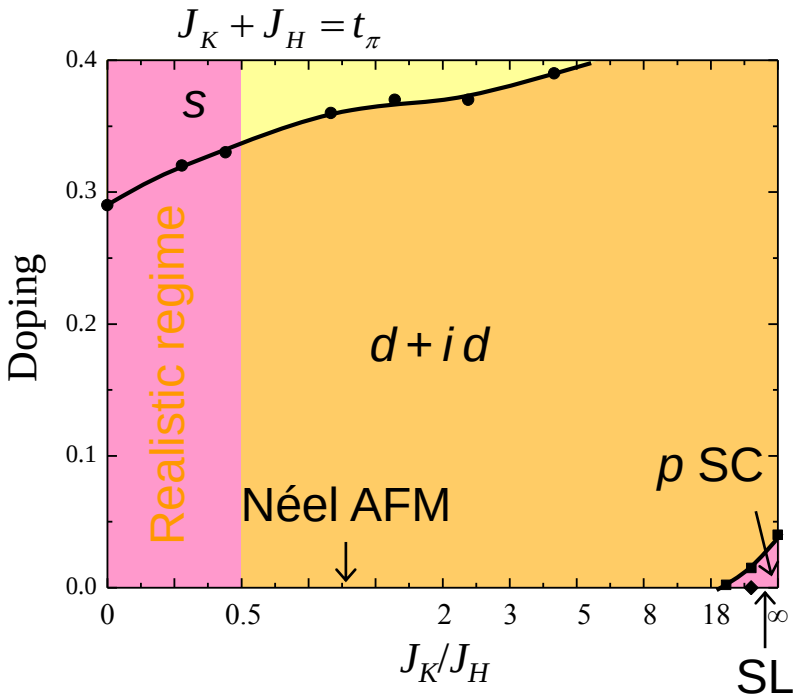

C.f., *d*(x^2-y^2)-wave SC in doped Sr2IrO4; Wang and Senthil, PRL **106**, 136402 (2011), Watanabe et al., PRL **110**, 027002 (2013), Meng, Kim, Kee, PRL **113**, 177003 (2014).

- Broken time-reversal symmetry in *d*+*id* SC, *p* SC

***d* + *i d*:**

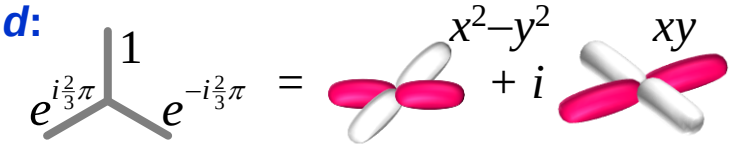

As in *tJ* model on honeycomb lattice

Black-Schaffer and Doniach, PRB **75**, 134512 (2007). Talk by Le Hur (July 24).

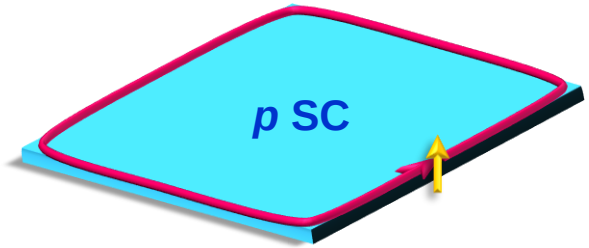

Similar *p* SC in a doped FM Kitaev model by You, Kimchi, and Vishwanath, PRB **86**, 085145 (2012).

Spin-charge-Chern liquid at n=1/4, Jiang, Mesaros, Ran, PRX **4**, 031040 (2014); Talk by Y. Ran (July 21).

- **Realistic regimes are very similar to the doped *tJ* model on a honeycomb lattice.**
- **Other systems may show even more exotic phases (not fully explored).**

SU(2) slave-boson mean-field phase diagram for Kitaev-Heisenberg model

SO, PRB **87**, 064508 (2013).

$$H = -t\sum_{\langle ij\rangle\sigma}\left(\tilde{c}^{\dagger}_{i\sigma}\tilde{c}_{j\sigma} + h.c.\right) + H_K + H_H$$

$$|J_K| + |J_H| = 2t = 2$$

- Broken time-reversal symmetry in p SC$_1$, d+id SC, and FM

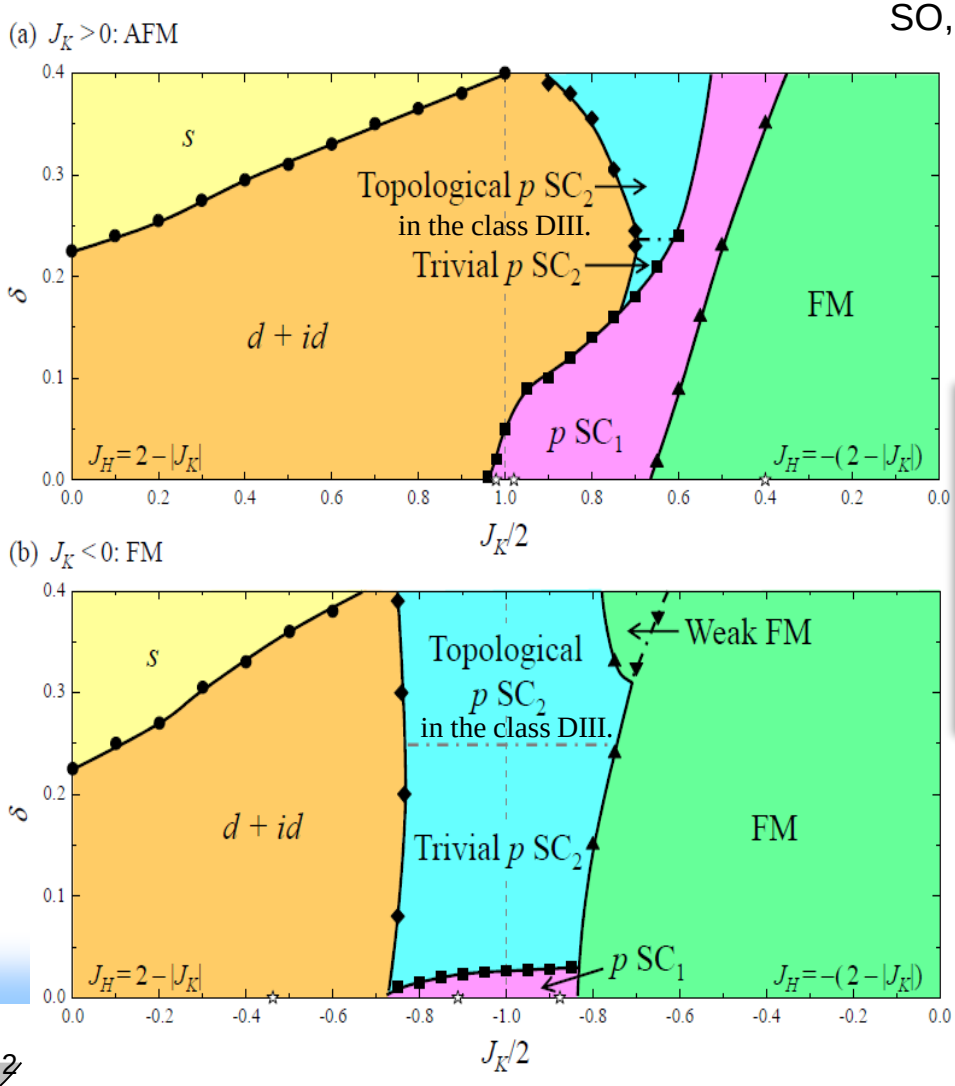

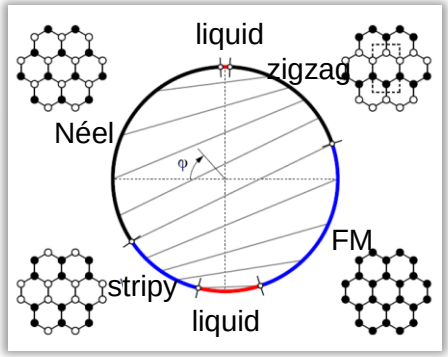

Chalopuka *et al.*, PRL **110**, 097204 (2013).

p SC$_2$: Hyart *et al.*, PRB **85**, 140510 (2012)

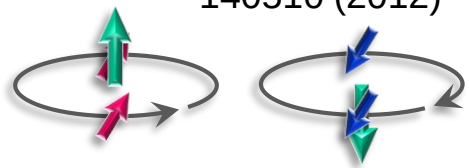

c.f., B-phase of superfluid ^{3}He

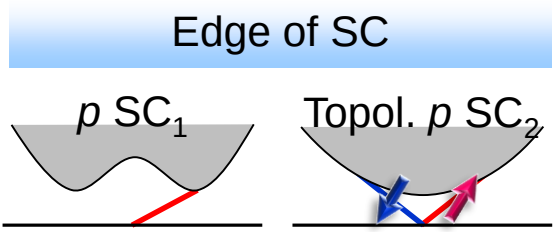

FM Kitaev & AFM Kitaev models are quite different when carriers are doped.

- **Possibility of exotic SC states**
- **Materials realization?**

Summary

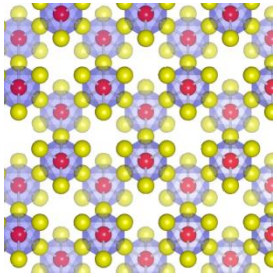

Theoretical proposal:
Designing novel quantum phenomena in (111) bilayers of perovskite transition metal oxides

1. Mimic graphene
2. Locate the Fermi level at Dirac points
3. Turn on the spin-orbit coupling

- (111) bilayer of $LaAuO_3$ is a good candidate for a 2-dimensional topological insulator.

  Nat. Commun. **2**, 596 (2011).

- (111) bilayer of $SrIrO_3$ is on the verge of a correlation-induced Mott transition, and it is most likely an AF trivial insulator.

  Phys. Rev. B **89**, 195121 (2014)

- From strong coupling, low energy electronic states of $SrIrO_3$ bilayer are described by a Kitaev-Heisenberg model, and carrier doping may induce *d*+*id*-wave superconductivity.

  Phys. Rev. Lett. **110**, 066403 (2013).

- More interesting phenomena may be possible, topological Mott insulator, fractional QH, *etc*?
- Waiting for experimental realizations

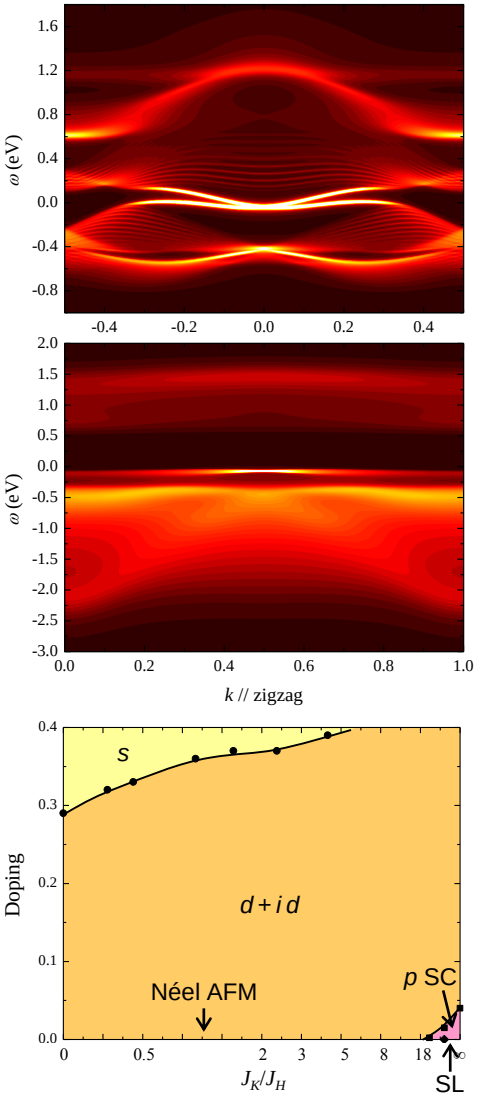

Incomplete list of related theoretical work

$LaNiO_3$ systems

- A. Rüegg and G. A. Fiete, PRB **84**, 201103(R) (2011).
- K.-Y. Yang, W. Zhu, D. Xiao, S.O., Z. Wang, and Y. Ran, PRB **84**, 201104(R) (2011).
- A. Rüegg, C. Mitra, A. A. Demkov, and G. A. Fiete, PRB **85**, 245131 (2012); **88**, 115146 (2013).
- D. Doennig, W. E. Pickett, and R. Pentcheva, PRB **89**, 121110(R) (2014).

$SrTiO_3$ systems

- D. Doennig, W. E. Pickett, and R. Pentcheva, PRL **111**, 126804 (2013).

$SrIrO_3$ systems "Topological semimetal" not AF trivial ins.

- J. L. Lado, V. Pardo, and D. Baldomir, PRB **88**, 155119 (2013).

$La(Ni,Co)O_3$ systems

- B. Ye, A. Mesaros, and Y. Ran, PRB **89**, 201111 (2014).
- Y. Wang, Z. Wang, Z. Fang, and X. Dai, PRB **91**, 125139 (2015).

$LaAuO_3/LaCrO_3$ systems

- X. Hu, Adv. Matter. **24**, 294 (2012).
- Q.-F. Liang, L.-H. Wu, and X. Hu, NJP **15**, 063031 (2013).

Double perovskite Sr_2FeMoO_6

- A. M. Cook and A. Paramekanti, PRL **113**, 077203 (2014).

"Dice" lattice: (111) trilayer

- F. Wang and Y. Ran, PRB **84**, 241103(R) (2011).

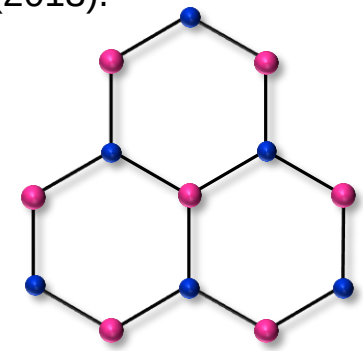

Buckled honeycomb
(111) bilayer

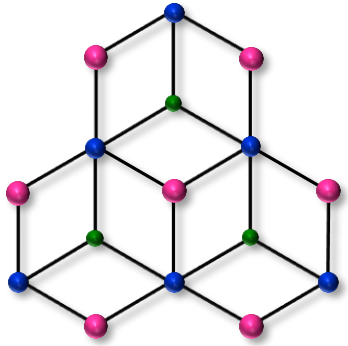

Dice
(111) trilayer

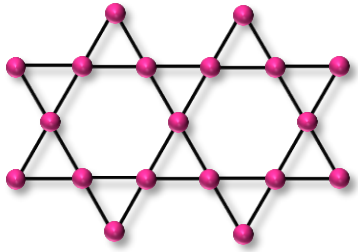

Kagomé
(111) Monolayer of pyrochlore

(111) family

Pyrochlore oxides

- X. Hu, A. Rüegg, G. A. Fiete, PRB **86**, 235141 (2012).
- E. J. Bergholtz, Z. Liu, M. Trescher, R. Moessner, and M. Udagawa, PRL **114**, 016806 (2015).
- Chen, Hung, Hu, Fiete, arXiv:1504.03646.

Very recent experimental result
Talk by Takagi-sensei

APL Materials **3**, 041508 (2015)

Fabrication of (111)-oriented $Ca_{0.5}Sr_{0.5}IrO_3/SrTiO_3$ superlattices—A designed playground for honeycomb physics

Daigorou Hirai,[1] Jobu Matsuno,[2] and Hidenori Takagi[1,3]
[1]*Department of Physics, University of Tokyo, Hongo 7-3-1, Bunkyo-ku, Tokyo 113-0033, Japan*
[2]*RIKEN Center for Emergent Matter Science (CEMS), Wako, Saitama 351-0198, Japan*
[3]*Max-Plank-Institute for solid state research, Heisenbergstrasse 1, Stuttgart 70569, Germany*

(Received 7 January 2015; accepted 11 February 2015; published online 24 February 2015)

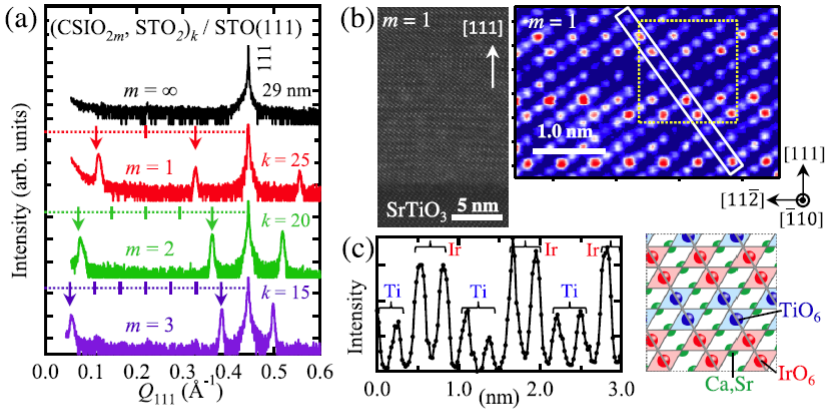

FIG. 3. (a) X-ray diffraction θ-2θ scans for the superlattice $[(Ca_{0.5}Sr_{0.5}IrO_3)_{2m},(SrTiO_3)_2]_k$ on $SrTiO_3(111)$ with $m = 1$, 2, 3, and ∞. Superlattice reflections are indicated by arrows. (b) Atomically resolved HAADF-STEM image of the superlattice with $m = 1$ along the $SrTiO_3$ [111] direction. (c) Left panel; intensity scan along the column indicated in the HAADF-STEM image shown in (b). Right panel; schematic illustration of stacking of IrO_6 and TiO_6 (111) bilayers in the dotted square in (b).

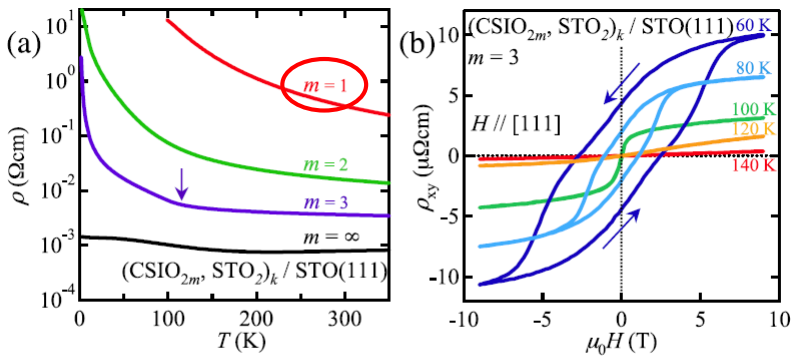

FIG. 4. (a) Temperature dependence of resistivity $\rho(T)$ for the superlattice $[(Ca_{0.5}Sr_{0.5}IrO_3)_{2m},(SrTiO_3)_2]_k/SrTiO_3(111)$ with $m = 1$, 2, 3, and ∞. A kink in the resistivity curve for the $m = 3$ superlattice is indicated by an arrow. (b) Hall resistivity (ρ_{xy}) of the $m = 3$ superlattice at various temperatures is plotted as a function of applied field.

$Ca_{0.5}Sr_{0.5}IrO_3$ (111) bilayer is strongly insulating (with magnetic ordering).

(111) trilayer, quadralayer, *etc*, of $SrIrO_3$ and (111) bilayer of $SrRhO_3$ should be examined using DFT+DMFT?

Acknowledgement

Di Xiao
Carnegie Mellon University

Ying Ran
Boston College

Wenguang Zhu
University of Science and Technology of China

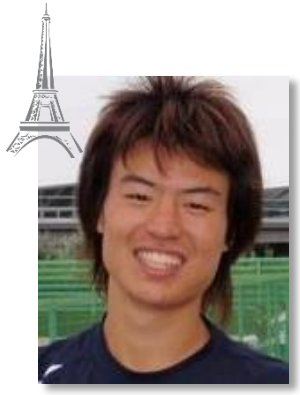

Yusuke Nomura
University of Tokyo
(Moved to Biermann's group)

Ryotaro Arita
RIKEN

Naoto Nagaosa
RIKEN
University of Tokyo

Special thanks

IMR Tohoku University
Institute for Materials Research, Tohoku University